Chemical Reactor Network Targeting and Integration: An Optimization Approach

Subash Balakrishna* and Lorenz T. Biegler

Chemical Engineering Department
Carnegie Mellon University
Pittsburgh, Pennsylvania

While synthesis strategies are well developed for energy integration and separation systems, relatively little work has been done in synthesizing reactor networks. This is due to the complex and nonlinear behavior of the reacting system, coupled with the combinatorial aspects inherent in all synthesis problems. This paper provides a brief summary of work to date in this area, focusing on targeting approaches for reactor network synthesis.

*Currently with Mobil Corporation, Beaumont, Texas.

ADVANCES IN CHEMICAL ENGINEERING, VOL. 23

As with energy integration, reactor network targeting seeks to describe the performance of the network without its explicit construction. Once this description has been obtained, a network is then determined that is guaranteed to match this target. To achieve these objectives, we rely on recent concepts of attainable regions and extend these to simple optimization formulations. With these formulations, network targets can be achieved for isothermal and nonisothermal systems with complex kinetics.

Moreover, these optimization formulations can easily be coupled to other process systems such as heat integration and separation sequences. As a result, they provide a framework for integrated process design. This strategy is illustrated with detailed examples. Finally, limitations of the current approach are summarized and topics for future work are outlined.

I. Introduction

Synthesis of chemical reactor networks can be defined by the following problem statement:

Given the reaction stoichiometry and rate laws, a desired objective and system constraints, what is the optimal reactor network structure? What is the flow pattern of this network? Where should mixing or segregatation occur in this network? Where should heating and cooling be applied in this network?

Despite significant research, both in reactor modeling and analysis and in the design of specific reactors, relatively little work has been reported in reactor network synthesis. As noted in the process synthesis review of Nishida *et al.* (1981), other areas of process synthesis, including heat integration and separation synthesis, have advanced much more than reactor networks. Several reasons account for this. First, reacting systems are typically more difficult to model, and they generally have more diverse elements than energy or separation systems. This is typified by an important (and expensive) experimental component. Moreover, given the resource constraints in process development, there is often little opportunity to find an optimal reactor network by developing a detailed reactor model or by investigating many possible alternatives.

Nevertheless, as noted by Douglas (1988), the reactor system is often the heart of the chemical process, as it dictates the downstream processes (e.g., separation and waste treatment) and strongly influences both the recycle and separation structures as well as the energy network. Despite this, the general approach is to design the reactor system "in isolation" and then to design the

remaining subsystems. As will be seen in this paper, these "sequential" approaches are clearly suboptimal, and large improvements in the overall process can be made through process integration. It is also hoped that these case studies will encourage the development of more detailed models for reactor targeting at the design stage.

Previous work in reactor network synthesis can be summarized from various sources. First, most textbooks on reactor design (e.g., Levenspiel, 1962; Kramers and Westerterp, 1963; Froment and Bischoff, 1979; Fogler, 1992) present graphical and heuristic approaches that emphasize the effects of mixing for various reaction orders and heating for exothermic and endothermic reactions. These methods are then used to guide the selection of ideal reactors [e.g., plug flow (PFR) and continuous stirred tank (CSTR) reactors]. However, these approaches are usually limited to single reactions or simple series/parallel cases. While these heuristics can also be applied to more complex problems, a quantitative evaluation of trade-offs is often required and considerably more effort is introduced if an optimal network is desired.

Early studies that applied systematic optimization approaches can be classified as optimal control studies and superstructure optimization. Studies based on the former include the use of adjoint variables and sensitivities by Horn and Tsai (1967), the development of adjoint networks for reacting streams by Jackson (1968), and its extension to include CSTRs by Ravimohan (1971). Paynter and Haskins (1970) attempted to formulate the selection of CSTRs and PFRs through optimal controls for axial dispersion (ADR) models, and Waghmere and Lim (1981) related CSTR/PFR selection to optimal profiles in batch and semibatch reactor systems. Achenie and Biegler (1986) modified the approach of Jackson to use ADRs as well in order to aid in CSTR/PFR selection. Later, they developed an optimal control formulation (Achenie and Biegler, 1988) based on transfer from segregated flow to maximum mixing compartments. In addition to these general network studies, there are numerous optimal control studies related to specific reactor systems (e.g., Glasser *et al.*, 1987; Jackson, 1968; Dyson and Horn, 1967; Narasimhan, 1969).

The structural optimization of superstructures can probably be traced to Aris (1961), who applied dynamic programming to a series of reactors. This approach was advanced and summarized by Hartmann and Kaplick (1990) and extended through optimization of serial recycle reactors by Chitra and Govind (1985). More efficient uses of nonlinear programming to solve superstructure problems were also developed by Pibouleau *et al.* (1988) and Achenie and Biegler (1990). Among the superstructure approaches, several studies by Kokossis and Floudas (1989, 1990, 1991) applied sophisticated mixed-integer nonlinear programming (MINLP) strategies to a large reactor network. Modeled as CSTRs or a series of sub-CSTRs that represented PFRs, this MINLP problem was capable of handling arbitrary kinetics for both isothermal and nonisothermal cases. In addition,

these authors demonstrated the interaction of this network with other parts of the process flowsheet. Finally, they also incorporated stability constraints within the MINLP problem in order to avoid the selection of unstable network structures.

While these optimization-based approaches have yielded very useful results for reactor networks, they have a number of limitations. First, proper problem definition for reactor networks is difficult, given the uncertainties in the process and the need to consider the interaction of other process subsystems. Second, all of the above-mentioned studies formulated nonconvex optimization problems for the optimal network structure and relied on local optimization tools to solve them. As a result, only locally optimal solutions could be guaranteed. Given the likelihood of extreme nonlinear behavior, such as bifurcations and multiple steady states, even locally optimal solutions can be quite poor. In addition, superstructure approaches are usually plagued by the question of completeness of the network, as well as the possibility that a better network may have been overlooked by a limited superstructure. This problem is exacerbated by reaction systems with many networks that have identical performance characteristics. (For instance, a single PFR can be approximated by a large train of CSTRs.) In most cases, the simpler network is clearly more desirable.

For the above reasons, we instead develop in this paper an approach based on reactor network targeting. Here, we develop simplified optimization formulations that accurately predict network performance prior to their construction. This approach is based on geometric concepts for attainable regions (AR) of the reactor network initially developed by Glasser *et al.* (1987). In Section II, we describe and summarize the geometric properties that relate to the attainable region. In Section III, these are applied to develop optimization formulations for isothermal systems, and Section IV extends these formulations to nonisothermal system. Sections V and VI then describe the integration of reactor targeting optimization problems with energy and separation systems, respectively. Finally, Section VII summarizes the paper and outlines areas for future work.

II. Geometric Concepts for Attainable Regions

For chemical reactor networks, the attainable region concept was first defined by Horn (1964), who noted that

> [V]ariables such as recycle flow rate and composition of the product form a space which in general can be divided into an attainable region and a non-attainable region. The attainable region corresponds to the totality of physically possible reactors. . . . Once the border is known the optimum reactor corresponding to a certain environment can be found by simple geometric considerations.

To illustrate this concept, consider the attainable region for the following series reaction:

$$A \rightarrow B \rightarrow C$$

which can be defined in the space of concentrations for A and B as shown in Fig. 1. Here, we assume a fixed feed and initial temperature and trajectories that are determined entirely by the state equations for concentration. (This is true in steady state for isothermal or adiabatic systems.) With this attainable region, we clearly see that point *F* and the line segment *GH* represent the maximum concentration of B and maximum selectivity of B to C, respectively. These can be achieved by the reactor networks needed to construct the attainable region boundary. Moreover, if a more complex objective represented in terms of C_A and C_B yields an interior optimum point, then again this point can be achieved by any linear combination of the boundary structures.

We construct the attainable region by noting that the concentration space is a vector field with a rate vector (e.g., in Fig. 1, $dC_B/dC_A = R_B/R_A$) defined at each point. Moreover, we are not restricted to concentration space, but can consider any other variable that satisfies a linear conservation law (e.g., mass fractions, residence time, energy, and temperature—for constant heat capacity and density). The attainable region is an especially powerful concept; once it is known, performance of the network can often be determined without the network itself.

More recently, Glasser *et al.* (1987) developed geometric properties of the attainable region along with a constructive approach for determining this region. They defined the necessary conditions for the attainable region as follows:

(1) The attainable region (AR) must be convex. Any point created by a linear combination of two points in the AR must be in the AR, as it can be

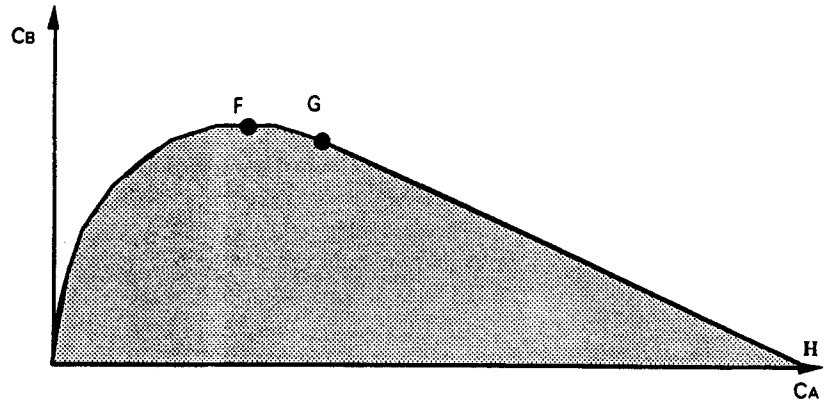

FIG. 1. Attainable region in concentration space.

created by mixing these two points. Moreover, this property ensures that the AR cannot be extended by further mixing.

(2) No reaction vector in the AR boundary can point out of the AR. If this were the case, the AR could be extended further by PFR reactors, which have trajectories that are always tangent to the rate vectors.

(3) No reversed reaction vector in the complement of the AR can point back into the AR. Note that a CSTR can be represented in the AR by a line with ends at the feed and outlet concentrations, with the rate vector at the CSTR outlet collinear with this line. Thus, this condition ensures that the AR cannot be extended further by a CSTR.

These properties hold for all dimensions and are, in fact, stronger than the simple exclusion of CSTRs, PFRs, and mixing. Hildebrandt (1989) proved that an AR closed to further extension by PFRs and CSTRs is also closed to extension by recycle PFRs (RRs) as long as the AR is not constrained in concentration. Hildebrandt *et al.* (1990) also showed how these properties could be applied to systems with nonconstant densities and heat capacities.

These concepts can also be shown to apply to the more general case where the reacting system is described by

$$dC/d\tau = R(C) + q(C_0 - C)$$

where C_0 is an arbitrary concentration and $q(\tau)$ represents the sidestream flowrate. In addition to the limiting cases of PFRs ($q = 0$), CSTRs ($dC/d\tau = 0$), and pure mixing ($q = \infty$), we can also consider differential sidestream reactors (DSRs), the maximum mixed case discussed by Zwietering (1959). Finally, Hildebrandt and Feinberg (1992) have shown that the AR itself consists of PFR surfaces and straight-line segments. If the intersection of these surfaces and straight lines—called a *connector*—is smooth, it defines a DSR with a feed point at C_0.

If the problem can be modeled in two concentration dimensions, the connector is simply a point and this line–surface intersection can be represented by a simple CSTR at C_0. Thus, DSRs are not necessary for the construction of a two-dimensional AR. In fact, two-dimensional systems allow for a straightforward algorithm for the construction of the AR, based on tracing alternating PFR and CSTR trajectories until the necessary conditions are satisfied. Here, we begin with a PFR trajectory from the feed point and trace it to its equilibrium point. Any nonconvexities in the region are then filled in with straight-line segments to form a convex hull. If any rate vectors point out of the straight line segments, we know that the AR can be extended by a CSTR; we thus find a CSTR with feed on the PFR trajectory that extends the AR the most. Any nonconvexities in this trajectory are again filled in with line segments, and we

continue until there are no further rate vectors pointing out from the straight-line segments. From the outlet of the (boundary) CSTR, we then trace the PFR trajectory to its equilibrium point, continue to fill in nonconvexities, and apply the above steps until the necessary AR conditions are satisfied.

Glasser *et al.* (1987) and Hildebrandt *et al.* (1990) demonstrated this two-dimensional approach on a number of small reactor network problems, with better results than previously reported. Moreover, Omtveit and Lien (1993) were able to consider higher-dimensional problems as well through projections in concentration space that allow a complete two-dimensional represention. These projections were accomplished through the principle of reaction invariants (Fjeld *et al.,* 1974) and the imposition of system specific constraints.

For three dimensions, the AR construction algorithm is similar to the one described above—with the added possibility that we can find a (one-dimensional) connector on the AR that is described by a DSR. Glasser *et al.* (1992) defined conditions under which DSRs appear on the AR along with a direct method for finding the feed addition rate, q. While the conditions for DSRs appear to occur infrequently, examples have been constructed in the space of conversion, temperature, and residence time where the DSR was a prominent part of the AR. Nevertheless, Hildebrandt and co-workers conclude that most ARs will consist only of CSTR and PFR surfaces. In dealing with n-dimensional problems, Hildebrandt and Feinberg noted that the AR boundary is defined by line segments and PFR trajectories, with at most n structures needed to define a point on the AR boundary and $n + 1$ structures needed to define an interior point of the AR. Thus, for three-dimensional problems, at most three parallel structures (PFRs, CSTRs, DSRs) are needed to define any AR boundary point.

Finally, the AR concept can be extended beyond regions that are closed to further mixing and reaction. Godorr *et al.* (1994) have also considered multirate processes where, for example, a mixture of catalysts will lead to a superposition of two separate reaction mechanisms. These authors also considered operations of mixing, condensing, and boiling as well as separation coupled with reaction. Here, they modified the concept of connectors to accommodate multiple rates and hence create more appropriate attainable regions. However, the graphical procedure for constructing ARs has limitations beyond three dimensions, as it requires an inspection of all the boundary points. Thus, the attainable region concepts need to be combined with more powerful, higher-dimensional search procedures. Hildebrandt and Biegler (1994) presented a discussion of these concepts and the role of optimization formulations for higher-dimensional search and for integration of the reactor targeting procedure with other process subsystems. In the next sections we further develop and review these AR optimization formulations, based on the recent work of Balakrishna and Biegler (1992a, 1993).

III. Reactor Network Synthesis: Isothermal Systems

In this section, we develop a simple and efficient formulation for target-based reactor synthesis for homogeneous, constant-density reacting systems. As described in Section I, previous superstructure and target-based approaches have many limitations. In superstructure-based approaches, the solution is only as rich as the superstructure chosen; moreover, these approaches usually suffer from local and nonunique solutions which are characteristic of reactor networks. By combining AR concepts and optimization formulations, we instead create targets for this network through the solution of simple optimization problems. Unlike the geometric approach to finding an AR, optimization approaches, in principle, do not have a dimensionality limitation.

A. The Segregated-Flow Approximation

Given the reaction stoichiometry and rate laws for an isothermal system, a simple representation for targeting of reactor networks is the segregated-flow model (see, e.g., Zwietering, 1959). A schematic of this model is shown in Fig. 2. Here, we assume that only molecules of the same age, t, are perfectly mixed and that molecules of different ages mix only at the reactor exit. The performance of such a model is completely determined by the residence time distribution function, $f(t)$. By finding the optimal $f(t)$ for a specified reactor network objective, one can solve the synthesis problem in the absence of mixing.

The isothermal formulation for maximizing the performance index in segregated flow is given by

$$
\begin{aligned}
\underset{f(t)}{\text{Max}} \quad & J(X_{\text{exit}}, \tau) \\
& \frac{dX_{\text{seg}}}{dt} = R(X_{\text{seg}}) \\
& X_{\text{seg}}(0) = X_0 \\
& X_{\text{exit}} = \int_0^{t'_{\max}} f(t)\, X_{\text{seg}}(t)\, dt \\
& \int_0^{t'_{\max}} t\, f(t)\, dt = \tau \\
& \int_0^{t'_{\max}} f(t)\, dt = 1
\end{aligned}
\tag{P1}
$$

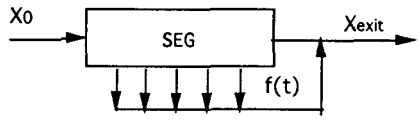

FIG. 2. Segregated-flow model.

Here, X_{seg} is the dimensionless concentration vector (normalized, e.g., by a feed concentration), $R(X)$ is the corresponding rate vector, and X_{exit} is the dimensionless output concentration of the segregated flow system with a residence time τ. We allow the objective function, J, to be specified by the designer as any function of X_{exit} and τ. One can see that the differential equation system can be uncoupled from the rest of the model and solved offline if the dimensionless feed concentration, X_0, is prespecified. Once the vectors X_{seg} are determined, we merely solve for $f(t)$, which satisfies an additional set of linear constraints. If Gaussian quadrature on finite elements is applied to the above model over the domain $[0, t_{max}]$, we get

$$\begin{aligned} \underset{f_{(i,j)}}{\text{Max}} \quad & J(X_{exit}, \tau) \\ & \sum_i \sum_j w_j f_{(i,j)} \Delta\alpha_{(i)} = 1 \\ & \tau = \sum_i \sum_j w_j f_{(i,j)} t_{(i,j)} \Delta\alpha_{(i)} \\ & X_{exit} = \sum_i \sum_j w_j f_{(i,j)} X_{seg\ (i,j)} \Delta\alpha_{(i)} \end{aligned} \tag{P2}$$

where

i = Index set of finite elements
j = Index set of Gaussian quadrature (or collocation) points
$f_{(i,j)}$ = RTD function at jth quadrature point in ith element (point $[i,j]$)
$X_{seg(i,j)}$ = Dimensionless concentration at point $[i,j]$
w_j = Weights of Gaussian quadrature
$\Delta\alpha_i$ = Length of ith finite element (fixed)

It is clear that the above formulation is linearly constrained in $f_{(i,j)}$ and the solution of (P2) gives us a global optimum in segregated flow for any concave objective function. Moreover, we can reduce this problem to a linear program for both yield and selectivity objective functions by applying suitable transformation techniques (Balakrishna, 1992). Then we can solve the problem by any linear programming algorithm.

The solution to this problem provides a good lower bound for the targeting problem. Also, the segregated flow model is often sufficient for the reactor synthesis problem. The solution to this simple formulation thus could be chosen

to represent the first stage in an iterative synthesis approach. Before constructing this procedure, we first develop conditions under which the segregated-flow model is itself sufficient for the reactor synthesis problem.

B. Sufficiency Conditions for Segregated-Flow Networks

The segregated-flow model described by (P2) forms a basis to generate an AR. We now develop conditions for the closure of this space with respect to the operations of mixing and reaction by means of a PFR, a CSTR, or a recycle PFR (RR). Consider the region depicted by the constraints of (P2). Our aim is to develop conditions that can be checked easily for the reaction system in question so that, if these conditions are satisfied, we need to solve only (P2) for the reactor targeting problem. We will analyze these conditions based on PFR trajectories projected into two dimensions. Here, a PFR, which is an n-dimensional trajectory in concentration space and parametric in time, is generated by the solution of the initial value differential equation system in (P1). Figure 3 illustrates a PFR trajectory and its projections in three-dimensional space, where the solid line represents the actual PFR trajectory and the dotted lines represent the projected trajectories.

Consider a reaction system consisting of a set of components $i = 1, 2, ..., n$. Associated with each is a reaction rate r_i. Let $I = \{i\}$ denote the complete set of reacting species. This set can be further classified into

$$I_1 = \{a\} = \{a \in I : r_a \leq 0\}$$

$$I_2 = \{j\} = \{j \in I : r_j \geq 0\}$$

$$I_3 = \{k\} = \{k \in I : r_k >,< 0\}$$

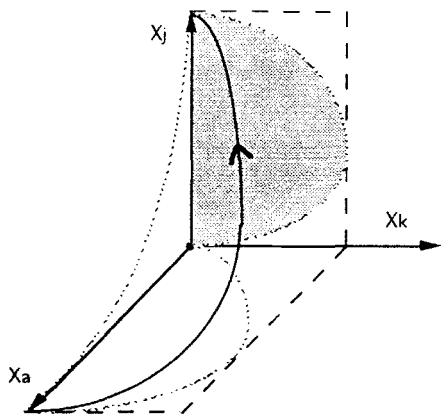

Fig. 3. An example of a PFR trajectory (solid line) and its projections (dotted lines).

In the most common case, our objective function is an explicit function of elements of I_3, which represent products of the reacting system. For completeness of segregated-flow systems, we are able to state the following properties, which are proved in Balakrishna and Biegler (1992a):

Property 1. *If the projected (onto R^2) PFR trajectories are such that $\{X_i : i \in I_1, I_3\}$ encloses a convex region with respect to any element of $\{X_a : a \in I_1\}$ and no two PFR projections meet within the bounds of possible concentrations, then none of these projected (two dimensional) spaces can be extended under the operations of mixing, additional PFRs/CSTRs/RRs, or any combination of these. This convex region implies that the projected curve is a concave function, $\partial^2 X_i/\partial X_a{}^2 \leq 0$.*

Corollary 1. *For any system that satisfies the conditions of Property 1, any reactor starting from the projected space will have an outlet concentration such that*

$$\frac{\Delta X_i}{\Delta X_a} \geq \frac{r_{i0}}{r_{a0}}$$

where ΔX_i is the change in concentration of component i accomplished by the reactor, ΔX_a is the corresponding change in the concentration of A, and r_{i0} and r_{a0} are reaction rates at the reactor inlet.

On the other hand, if the X_i vs. X_a curves are convex ($\partial^2 X_i/\partial X_a{}^2 \geq 0$) but still satisfy the condition that no two PFR projections meet, then the inequality above is reversed.

At this point, the utility of this property with respect to (P2) deserves attention. A careful look at P2 reveals that the shaded region in the projected space (for example, the X_j–X_k space) is exactly the projection on the X_j–X_k space of the feasible region of P2. The concave PFR projection defines the concentrations in segregated flow, and the interior is a convex combination of all boundary points created by the *residence time distribution* function. This gives a new interpretation to the residence time distribution as a convex combiner. For any convex objective function to be *maximized,* the solution to the segregated flow model will always lead to a boundary point of the AR.

Since we have closed-form expressions for the rate equations that form the tangents to the trajectories in concentration space (although we do not have closed-form expressions for the trajectories themselves), checking for concavity of the curves is easy. However, it is clear that we require certain convexity properties among the projections; i.e, we need to know *a priori* whether certain projected regions are convex. This task can be simplified by developing certain properties for mutual convexity in the reacting system.

Property 2. *If the projection of any element of $\{X_j\}$ vs. $\{X_a\}$ defines a convex curve and the projection of any element of $\{X_k\}$ vs. $\{X_a\}$ defines a concave*

curve, then the projected curves of $\{X_k\}$ *vs.* $\{X_j\}$ *are concave up to the stationary point in this projection, and this stationary point is unique if the* X_k–X_a *projected curve is strictly concave.*

Corollary 2. *If the projections of* $\{X_j\}$ *vs.* $\{X_a\}$ *define concave curves and the projections of* $\{X_k\}$ *vs.* $\{X_a\}$ *define concave trajectories, then the projected curves of* $\{X_k\}$ *vs.* $\{X_j\}$ *are concave* beyond *the stationary point in this projection, and this stationary point is unique if the* X_k–X_a *projected curve is strictly concave.*

C. Optimization Formulations for Reactor Synthesis

The properties described above enable us to identify the nature of different projections and can be very useful, as shown in the example problems (Section III.D). It is essential to note, however, that Property 1 is only a sufficient condition, but not always necessary. In other words, the segregated-flow model can be optimal even if these conditions are not satisfied. If the segregated-flow region (for P2) is not sufficient, we generate optimization formulations for extending this region, by superimposing various reactors on the region provided by the linearly constrained formulation. The main idea for this approach is

Given a candidate for the AR, can extensions to this region be generated? If yes, then create the extension and, on its convex hull, check for further extensions that improve the objective function. This procedure is continued until there are no extensions that improve the objective function.

The main insight in this approach is that the residence time distributions (RTDs) lead to convex combinations and the region enclosed by the segregated flow model is always convex. The aim now is to develop an algorithm by which, given a candidate for an AR, we should be able to check whether it can be extended to our advantage. Here, we restrict ourselves to PFR, RR, and CSTR extensions only.

Consider the feasible region from (P2), a convex combination of the concentrations in segregated flow, as the first candidate for the AR. Each combination of the RTDs and the concentrations gives a unique point in the feasible region. The following subproblem can also be embedded within (P2) in order to check whether, starting from any feasible point, a reactor can provide an extension that gives a point outside of the region of P2. Here, we consider a recycle reactor extension, since it includes the PFR and CSTR extensions as special cases. Strictly speaking, recycle reactors do not form the boundary of an attainable region (Hildebrandt, 1989) as any AR extended by an RR can also be extended by a CSTR in the absence of constraints. Nevertheless, we use the RR formulation to simplify the algorithm. Additional formulations for purely CSTR or PFR extensions can also be developed along the same lines.

Recycle Reactor (RR) Extension: If $J_{rr} > J_{P2}$, then the recycle reactor provides an advantageous extension to the AR.

$$
\begin{aligned}
\text{Max} \quad & J_{rr}\,(X_{exit}) \\
& X_{P2} = \sum_i \sum_j w_j f_{(i,j)}\, X_{seg\ (i,j)}\, \Delta\alpha_{(i)} \\
& \frac{dX_{rr}}{dt} = R(X_{rr}) \\
& X_{rr}\,(t = 0) = \frac{R_e X_{exit} + X_{P2}}{R_e + 1} \\
& X_{exit} = \sum_i \sum_j w_j f_{r(i,j)}\, X_{rr\ (i,j)}\, \Delta\alpha_{(i)} \\
& \sum_i \sum_j w_j f_{(i,j)}\, \Delta\alpha_{(i)} = 1.0 \\
& \sum_i \sum_j w_j f_{r(i,j)}\, \Delta\alpha_{(i)} = 1.0 \\
& l \le X_{exit} \le u
\end{aligned}
\tag{P3}
$$

where

J_{rr} = Objective function at the exit of the recycle reactor extension
X_{rr} = Dimensionless concentrations within the RR extension
R_e = Recycle ratio
X_{exit} = Vector of reactor exit concentrations
f_r = Linear combiner of all the concentrations from the plug flow section of the recycle reactor

The first equation describes the concentrations available from segregated flow. The model equations for a recycle reactor starting from any feasible point are described by the second and third equations. The fourth equation gives the concentration at the exit of the recycle reactor. Here, the vectors l and u are lower and upper bounds, respectively, on the exit concentration vector. Thus, if $J_{rr} > J_{P2}$, then the recycle reactor provides an advantageous extension over (P2).

In addition, if any of the projections X_i vs. X_j ($j \in I_2$) are concave and if we wish to eliminate searching in the interior of these projections, we can always include the following inequality, which arises out of geometric arguments (Corollary 1):

$$
\frac{(X_{P2}{}^i - X_{exit}{}^i)}{(X_{P2}{}^j - X_{exit}{}^j)} \le \frac{R^i\,(X_{P2})}{R^j\,(X_{P2})}
$$

It is important to note that CSTR/PFR/RR extensions can be applied to any convex candidate region, not just the one defined by (P2). The residence time distribution can be used to generate the convex candidates. A sequence of convex hulls can be generated until the conditions for completeness are satisfied (i.e., there are no further extensions). The synthesis flowchart shown in Fig. 4 illustrates these ideas. In the algorithm, we initially check the possibility of global optimality for (P2). If this solution is suboptimal, a more complex model can be solved to give an updated optimal solution. Thus the new or updated convex

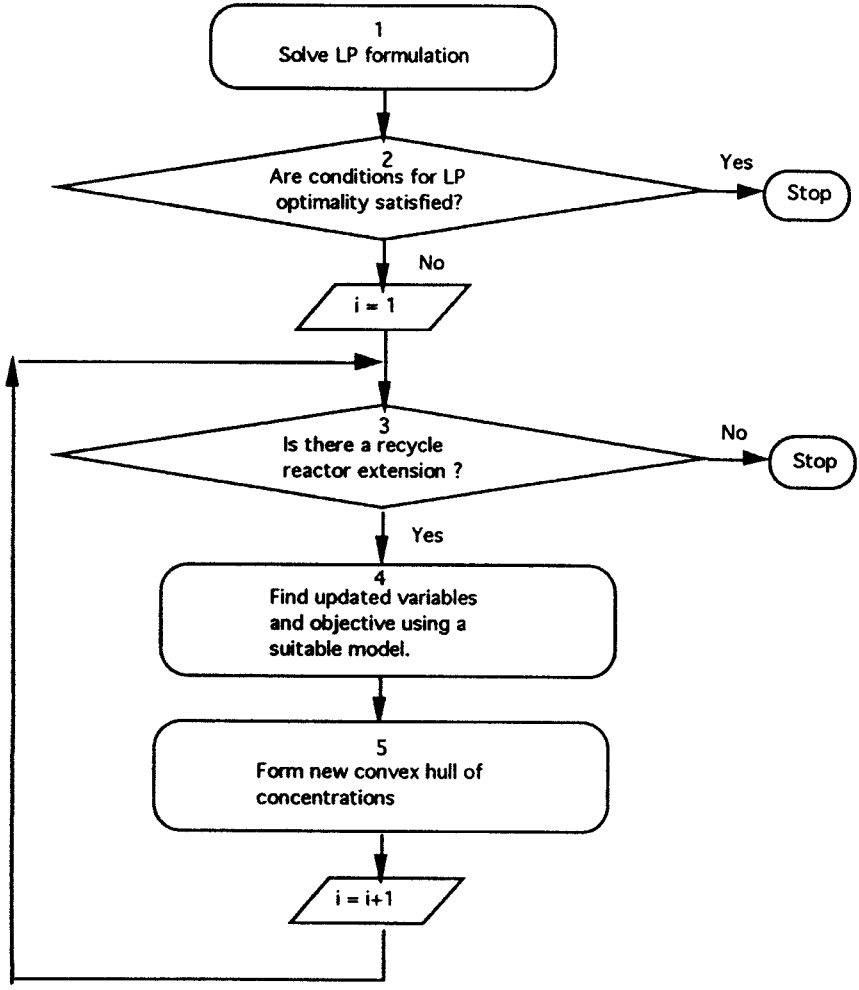

FIG. 4. Flowchart for stagewise synthesis.

hull based on the new concentrations can be generated, and the following subproblem, which represents Box 3 of the flowchart, can be solved.

$$\underset{R_e,\, f_{(i,j)},\, f_{\text{model}(k)}}{\text{Max}} \quad J(X_{\text{exit}})$$

$$\frac{dX_{\text{rr}}}{dt} = R(X_{\text{rr}})$$

$$X(t = 0) = \frac{R_e X_{\text{exit}} + X_{\text{update}}}{R_e + 1} \tag{P4}$$

$$X_{\text{update}} = \sum_i \sum_j f_{(i,j)} X_{\text{seg }(i,j)} + \sum_k f_{\text{model}(k)} X_{\text{model}(k)}$$

$$X_{\text{exit}} = \sum_i \sum_j f_{r(i,j)} X_{\text{rr}(i,j)}$$

$$\sum_i \sum_j f_{(i,j)} + \sum_k f_{\text{model}(k)} = 1.0$$

In this formulation, $X_{\text{model}(k)}$ is a constant vector and reflects the concentration at the exit in the models previously chosen. A convex combination of this with the segregated-flow region described by (P2) gives the fresh feed point for the recycle reactor we are looking for, X_{update}. Then X_{exit} represents the concentration at the exit of the recycle reactor; and if $J(X_{\text{exit}}) > J(X_{\text{model}(k)})$, the earlier model chosen is insufficient. The control variables essentially are the f's and $f_{\text{model}(k)}$, which are the linear combiners used to provide a convex candidate. A careful look at the formulation reveals that we are checking for completeness of the convex hull of the region found by the model.

Figure 5 gives a geometric interpretation to the solution of (P4). Here, if the solution of (P4) indicates that the objective function can be improved by extending the AR, e.g., based on segregated flow, we consider a more complex model. Thus, the expression for X_{update} automatically includes all the points in the convex hulls attained so far by previous recycle reactor extensions, and this region can be made up of the segregated-flow model as well as favorable recycle reactor extensions from previous solutions of (P4). We continue to check for extensions and terminate when there are no further extensions that improve the objective function. Note that with this approach, the algorithm allows the reactor network to be synthesized readily. It is also clear that this approach shares many characteristics with the geometric approach of Glasser *et al.* (1987). An important difference is that their approach searches for all possible extensions of candidate ARs and requires checking of an infinite number of points on the convex hull.

Our approach, on the other hand, automatically finds only those extensions that improve the objective function. Since it is an optimization-based approach, it is not limited, in principle, by problem dimensionality or the addition of

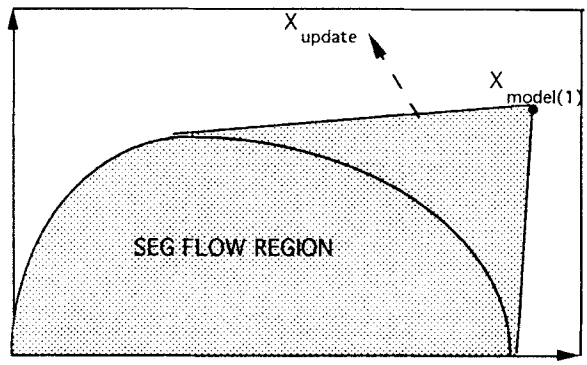

$X_{model(1)}$: Solution to first reactor extension from segregated flow.
X_{update} : Reactor Extension from combined hull of segregated flow and $X_{model(1)}$

FIG. 5. Extension of the convex hull (P4).

constraints, as will be demonstrated by the examples in the next section. We also note that because problems (P2) and (P4) are relatively small and simple optimization problems, AR solutions can be found very quickly.

One potential disadvantage to our optimization formulations, however, is that a particular extension that does not improve the objective function may still enlarge the AR enough so that a point from within this extension can improve the objective function beyond what we started with. This *nonmonotonic* increase in the objective is a limitation of the proposed approach. Also, we note that even though the attainable space of concentrations is always convex, (P4) is not necessarily a convex nonlinear program and therefore will not necessarily find the global optimum that we are seeking. However, termination at local optima is not always serious because the solution of (P2) usually yields an excellent starting point for (P4). (Also, multiple starting points could be tried to improve the likelihood of finding a global optimum for (P4).)

D. EXAMPLE PROBLEMS

We conclude this section with four example problems to illustrate our approach. The first problem satisfies the sufficiency conditions for segregated flow and is easily addressed by our approach. The second and third examples do not satisfy these properties but are readily solved by the algorithm of Fig. 4. Finally, the fourth example illustrates the difference between our optimization formulation and the geometric approach of Glasser *et al.* Several additional problems are also considered in Balakrishna and Biegler (1992a), with results superior to those presented in other articles.

Example 1. The isothermal van de Vusse (1964) reaction involves four species for which the objective is the maximization of the yield of intermediate species B, given a feed of pure A. The reaction network is given by

$$\begin{array}{ccccc} \mathrm{A} & \xrightarrow{k_1} & \mathrm{B} & \xrightarrow{k_2} & \mathrm{C} \\ {\scriptstyle k_3}\downarrow & & & & \\ \mathrm{D} & & & & \end{array}$$

Here, the reaction from A to D is second-order. The feed concentration is $c_{A0} = 0.58$ mol/liter and the reaction rates are $k_1 = 10\ \mathrm{s}^{-1}$, $k_2 = 1$, s^{-1} and $k_3 = 1$ liter g-mol^{-1} s^{-1}. The reaction rate vector for components A, B, C, and D, respectively is given in dimensionless form by:

$$R(X) = [-10X_A - 0.29X_A^2,\ 10X_A - X_B,\ X_B,\ 0.29X_A^2]$$

where $X_A = C_A/C_{A0}$, $X_B = C_B/C_{A0}$, and C_A, C_B are the molar concentrations of A and B, respectively. The objective function is the yield of component B. Following the algorithm in Fig. 4, we find that the solution of (P2), which is an LP, gives a globally optimal reactor network. This is because the reaction kinetics satisfy the conditions in Property 1 (i.e., the X_B vs. X_A curves are concave). The verification of concavity is simple, because we just have to verify the monotonicity of the slopes, given in closed form for the reactor synthesis problem. Here, the slope of the PFR trajectories in X_B vs. X_A space is just given by Rate(B) / Rate(A), and a simple program to find the maximum of the second derivative can be solved. The optimal value of the objective function is given by $X_B^{exit} = 0.7636$. This is the globally optimal solution and can be realized by a PFR with a residence time of 0.288 s. A brief comparison with results from the literature is presented below:

Study	Yield	Residence Time
Chitra and Govind (1985)	0.752	0.2551
Achenie and Biegler (1986)	0.7531	0.2965
Achenie and Biegler (1988)	0.757	0.2370
Kokossis and Floudas (1990)	0.752	0.2539
(P2) LP formulation	0.7636	0.2880

The results from the different approaches are nearly the same and differences could be attributed to numerical solutions of the PFR equations. The slightly better objective function predicted by the LP formulation may be due to a better approximation procedure when these differential equations are solved offline.

Example 2: The Trambouze reaction (Trambouze and Piret, 1959) involves four components and has the following reaction scheme:

$$\mathrm{A} \xrightarrow{k_1} \mathrm{B} \qquad \mathrm{A} \xrightarrow{k_2} \mathrm{C} \qquad \mathrm{A} \xrightarrow{k_3} \mathrm{D}$$

where the reactions are zero-order, first-order and second-order, respectively, with $k_1 = 0.025$ mol liter^{-1} min^{-1}, $k_2 = 0.2$ min^{-1}, $k_3 = 0.4$ liter mol^{-1} min^{-1}. We wish to maximize the selectivity of C to A defined by $X_C / (1 - X_A)$. Here the conditions of (P2) optimality are not satisfied; following the stagewise approach, we arrive at a CSTR extension from the feed point of the segregated-flow model, indicating a single CSTR with a selectivity of 0.5 and residence time of 7.5 s. No further extensions are observed by solving (P3). Achenie and Biegler (1990) observe a selectivity of 0.4999 in a two-CSTR combination. Kokossis and Floudas (1990) report many optimal networks to this problem with the same objective function of 0.5; Glasser *et al.* (1987) observe that this problem has an infinite number of optimal solutions with a selectivity of 0.5 in a CSTR with variable bypass.

Example 3: The α-pinene problem is a reaction network that consists of five species and has the following reaction network:

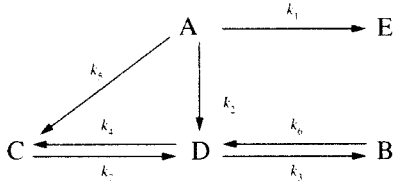

The objective function here is the maximization of the selectivity of C over D, given a feed of pure A.

The reaction vector for the components A, B, C, D, and E, respectively, is given by

$$R(X) = [-k_1 + k_2)X_a - 2k_5X_a^2, -k_6X_b + k_3X_d, k_5X_a^2 + k_4X_d^2 - k_7X_c, k_2X_a + k_6X_b - k_3X_d - 2k_4X_d^2 + 2k_7X_c, k_1X_a]$$

where $X_i = C_i/C_{A0}$ and $C_{A0} = 1$ mol/liter; $k_1 = 0.33384$ s^{-1}, $k_2 = 0.26687$ s^{-1}, $k_3 = 0.14940$ s^{-1}, $k4 = 0.18957$ liter mol^{-1} s^{-1}, $k_5 = 0.009598$ liter mol^{-1} s^{-1}, $k_6 = 0.29425$ s^{-1}, $k_7 = 0.011932$ s^{-1}.

This problem was solved by applying formulation (P2). Interestingly, the RTD always settles at the upper bound in the time horizon. Thus, we may infer that the selectivity in this problem increases monotonically with age within the segregated flow model. For instance, the selectivity obtained with a t_{max} of 60 s was 1.48. While this approach does not reveal the entire AR, this example corroborates some of the strengths of a target-based perspective that we mentioned earlier. Achenie and Biegler (1988) arrived at an optimal selectivity of 0.2336 by placing a bound on the residence time of 6 s. Kokossis and Floudas (1990), using a superstructure-based approach, arrived at a complex network of

a CSTR and a PFR (represented by sub-CSTRs) with recycles and intermediate feeds to get a maximum selectivity of 1.4020. Moreover, (P2) (an LP in this case) is based on a finite approximation to an infinite residence time domain. Thus, from the solution to our targeting model, it is easy to detect monotonicities in the objective function.

Example 4: Here, we revisit the van de Vusse reaction of Example 1 with altered rate constants. The objective function again is the yield of intermediate species B. The rate vector is given by $R(X) = [-X_A - 20X_A^2, X_A - 2X_B, 2X_B, 20X_A^2]$. In this case, the segregated-flow model gives a yield of 0.061. However, the sufficiency conditions for the LP formulation are not satisfied. Using our optimization formulation with recycle reactor extensions (P3), we observe a B yield of 0.069. Our network corresponds to a recycle reactor from the feed point (recycle fraction = 0.772; residence time in the plug section of RR = 0.1005 s) in series with a PFR with a residence time of 0.09 s. Glasser *et al.*, on the other hand, report a yield of 0.071 with a graphical approach. The lower yield obtained in this example can be attributed to a nonmonotonic increase in the objective, as mentioned earlier. It is interesting to note that if we apply the multicompartment approach of Achenie and Biegler (1988) to this problem, a yield of 0.0705 is obtained.

IV. Reactor Network Synthesis: Nonisothermal Systems

In this section, we develop a formulation for the synthesis of nonisothermal reactors, based on the isothermal targeting approach proposed in Section III. The targeting model is based on mixing between different reacting environments and is formulated as a dynamic optimization problem, where the temperature, the feed distribution function, and an exit flow distribution function are the control profiles. The optimization procedure results in the sequential solution of small nonlinear programming problems, where the solution to each NLP generates a component of the reactor network. This provides a constructive technique for the target-based synthesis of nonisothermal reactor networks for any general objective function and process constraints.

A. Nonisothermal Model Formulation

The targeting model for nonisothermal reactors derives much of its motivation from the targeting methodology described in the previous section. There, the only control profiles are the mixing functions (RTD) and we assumed that

mixing does not involve additional costs. In the case of nonisothermal systems, however, temperature is an added profile and we must consider the cost of maintaining this profile. One rather inexpensive technique for exothermic reactions is cold-shot cooling. However, mixing may not always be optimal in the space of concentrations, even if it is desirable in terms of temperature manipulation.

We therefore consider a different reaction flow model as our basic targeting model—one that can address temperature manipulation by feed mixing as well as by external heating or cooling. The model consists of a differential sidestream reactor (DSR), shown in Fig. 6, with a sidestream concentration set to the feed concentration and a general exit flow distribution function. (As mentioned in Section II, the boundary of an AR can be defined by DSRs for higher-dimensional (≥ 3) problems). We term this particular structure a *cross-flow reactor.* By construction, this model not only allows the manipulation of reactor temperature by feed mixing, but often eliminates the need to check for PFR extensions.

Figure 6 shows a schematic of a cross-flow reactor (CFR) with side exits, which we choose as our basic targeting model. Here, X_0 is the dimensionless concentration of the feed entering the reactor network, α is the independent variable denoting time as it progresses along the length of the reactor, and $T(\alpha)$ denotes the temperature as a function of the reactor length. We define $f(\alpha)\, d\alpha$ as the fraction of molecules in the reactor exit that leave between points α and $\alpha + \delta\alpha$ of the reactor (an exit flow distribution function), and $q(\alpha)$ as the probability density function for a molecule entering the system at point α in the reactor. Thus the number of molecules entering between points α and $\alpha + d\alpha$ is given by $q(\alpha)Q_0\, d\alpha$, where Q_0 is the flow rate entering the reactor network. Implicit in the formulation is the assumption of instantaneous mixing between the feed and the mixture in the reactor. In addition, the formulation can easily be extended for variable-density systems, although we consider only constant-density systems in this study.

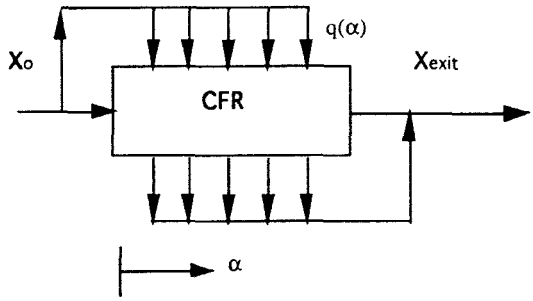

FIG. 6. General cross-flow reactor model.

Clearly, at one extreme—when $q(\alpha)$ is zero throughout the reactor and we have a general $f(\alpha)$—we have the equations for a segregated-flow model. On the other extreme—when $f(\alpha)$ is a Dirac delta exactly at one point and we have a general nonzero $q(\alpha)$—this model reduces to the Zwietering (1959) model of maximum mixedness. Also, we define $Q(\alpha)$ as the flow of molecules at point α. Based on this nomenclature, a differential mass balance on an element $\Delta\alpha$ leads to

$$\frac{dX}{d\alpha} = R(T(\alpha), X) + \frac{q(\alpha)Q_0}{Q(\alpha)}(X_0 - X(\alpha))$$

and with this governing equation in a cross-flow reactor, the mathematical model for maximizing the performance index in cross flow can be derived as follows:

$$\begin{aligned}
&\underset{q(\alpha),f(\alpha),T(\alpha)}{\text{Max}} \quad J(X_{\text{exit}}, \tau) \\
&\frac{dX}{d\alpha} = R(T(\alpha), X) + \frac{q(\alpha)Q_0}{Q(\alpha)}\ (X_0 - X(\alpha)) \\
&X(0) = X_0 \\
&X_{\text{exit}} = \int_0^\infty f(\alpha)X(\alpha)\, d\alpha \\
&\int_0^\infty f(\alpha)\, d\alpha = 1 \\
&\int_0^\infty q(\alpha)\, d\alpha = 1 \\
&\frac{Q(\alpha)}{Q_0} = \int_0^\infty [q(\alpha') - f(\alpha')]\, d\alpha' \\
&\int_0^\infty \int_0^\alpha [q(\alpha') - f(\alpha')]\, d\alpha'\, d\alpha = \tau
\end{aligned} \tag{P6}$$

Here, the last two equations define the flow rate and the mean residence time, respectively. This formulation is an optimal control problem, where the control profiles are $q(\alpha)$, $f(\alpha)$, and $T(\alpha)$. The solution to this problem will give us a lower bound on the objective function for the nonisothermal reactor network along with the optimal temperature and mixing profiles. Similar to the isothermal formulation (P3), we discretize (P6) based on orthogonal collocation (Cuthrell and Biegler, 1987) on finite elements, as the differential equations can no longer be solved offline. This type of discretization leads to a reactor network more

practically achievable than the schematic shown in Fig. 6 with a finite number of mixing points.

In the finite-element discretization, the subscript i denotes the ith finite element, and the subscript j (or k) denotes the jth (or kth) collocation point in any finite element. There are a total of N finite elements and K collocation points ($i = 1, N$; $j = 1, K$). The state variable X is approximated over each finite element by Lagrange interpolation basis functions ($L_k(\alpha)$) as:

$$X(\alpha) = \sum_{k=0}^{K} X_{ik} L_k(\alpha) \qquad \text{for } \alpha_{i0} \le \alpha \le \alpha_{i+1,0}$$

and

$$L_k(\alpha) = \prod_{l=0;k}^{K} \left[\frac{\alpha - \alpha_{il}}{\alpha_{ik} - \alpha_{il}} \right]$$

Substitution of this into (P6) leads to the following nonlinear program, the solution of which gives us the optimal control variables at the collocation points.

$$\begin{aligned}
&\underset{\phi_i,\ f_{ij},\ T_i}{\text{Max}} \quad J(X_{\text{exit}}, \tau) \\
&\sum_k X_{ik}\, L_k'(\alpha_j) - R(X_{ij}, T_{ij})\, \Delta\alpha_i = 0 \qquad j = 1, K \\
&X(0) = X_0 \\
&X_{i\text{end}} = \sum_k X_{ik}\, L_k(\alpha_{i+1}) \\
&X_{i,0} = \phi_i X_0 + (1 - \phi_i) X_{(i-1)\text{end}} \\
&X_{\text{exit}} = \sum_i \sum_j X_{ij} f_{ij} \qquad \text{(P7)} \\
&\sum_i \sum_j \alpha_{ij} (f_{ij} - q_{ij}) = \tau \\
&\sum_i \sum_j f_{ij} = 1 \\
&\phi_i Q_{i,1} = q_{i,1} Q_0 \\
&Q_{ij} = \sum_{ij} (q_{ij} - f_{ij}) Q_0 \\
&0 \le \phi_i \le 1
\end{aligned}$$

where

$L_k'(\alpha_j)$ = Derivatives of the Lagrange basis polynomials evaluated at α_j

ϕ_i = Ratio of the side inlet flow rate to the bulk flow rate within the reactor after mixing before element i

$\Delta\alpha_i = \alpha_{i+1,0} - \alpha_{i,0}$, the length of each finite element i

f_{ij} = Exit flow distribution at collocation point j in element i (point $[i,j]$)
q_{ij} = Fraction of inlet flow entering at $[i,j]$
T_{ij} = Temperature at $[i,j]$
X_{ij} = Dimensionless concentration at $[i,j]$
$X_{i\text{end}}$ = Concentration at end of ith finite element

Note that ϕ_i in this model is an approximation to

$$\frac{q(\alpha)Q_0}{Q(\alpha^+)} \qquad \left(\phi_i = \frac{q_i Q_0}{Q_{i,1}};\ Q_{ij} = \sum_{ij} (q_{ij} - f_{ij})Q_0\right)$$

and the equations in (P7) result from collocation applied to the differential equation model and Gaussian quadrature applied to the integral expressions. For convenience, the quadrature weights are absorbed into the respective discretized variables in the integration. Figure 7 is a schematic of this discretization.

Balakrishna (1992) has shown that if the finite elements ($\Delta\alpha_i$) are chosen sufficiently small, then (P7) simply reduces to a numerical scheme for solving (P6). Thus (P6) can now be solved as a nonlinear program to obtain the optimal set of f, T, and ϕ over each element. In this model, even though the temperature along the reactor is a control variable, part of the temperature manipulation can be readily accomplished by feed mixing if this is optimal for the reactor. In addition, the cross-flow reactor, by construction, mixes all available points on the reacting segments with the feed point, thus continuously checking for PFR extensions as long as the PFR trajectories are such that their nonconvexities can be enveloped from the feed point. These mixed points correspond geometrically to convex hulls; and since PFRs are already generated from these, there is often no need to check for the PFR extensions from the solution to the cross-flow reactor model.

B. Reactor Extensions

The solution to (P7) provides a lower bound to the performance index of the reactor network. In the case of purely isothermal reactors, we derive theoretical

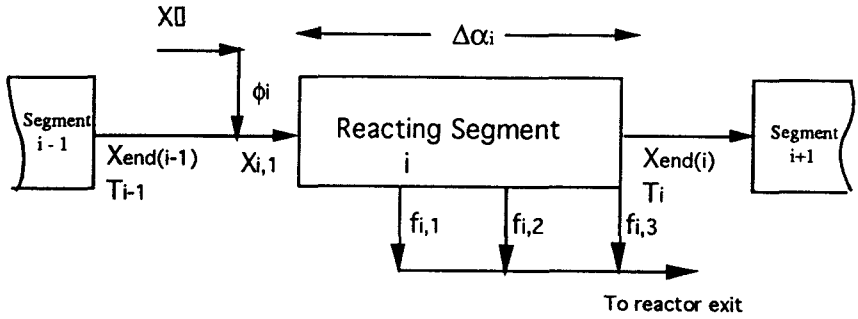

FIG. 7. Reactor representation for discretized cross-flow reactor model.

conditions of sufficiency for the segregated-flow model as in Section III, and we have checks for favorable extensions from the segregated-flow model, which are formulated as nonlinear programs. These results apply directly if the temperature profile can be related to the concentration profile (e.g., adiabatic reactors). However, more general nonisothermal reactors do not lend themselves to easy analysis owing to the assumption of a completely arbitrary temperature profile. Nevertheless, by applying the optimization formulations detailed in Section III, we can now develop techniques for extending the target provided by the CFR model. The constraints of (P7) define the feasible region for any achievable cross-flow reactor. The convex combination of all the concentrations in this region provides the entire region attainable by the cross-flow reactor and mixing, which corresponds to the first candidate for the AR. Based on the convex hull extensions illustrated in Section III, the following subproblem can be solved to check whether a reactor can provide an extension to the candidate AR. Here, we again consider a recycle reactor extension, since it includes the PFR and CSTR extensions as special cases. In the nonisothermal recycle reactor, we assume that the temperature is a control profile along the length of the plug flow section of the recycle reactor. The inlet temperature to the reactor that constitutes the extension will also follow a convex combination rule if intermediate heating or cooling is not permitted.

Recycle Reactor (RR) Extension: If $J_{rr} > J_{P7}$, then the recycle reactor provides an advantageous extension outside of A.

$$
\begin{aligned}
\text{Max} \quad & J_{rr}(X_{exit}, \tau_R) \\
& X_{P7} = \sum_i \sum_j \lambda_{ij} X_{cf}(i,j) \\
& \frac{dX_{rr}}{dt} = R(X_{rr}, T_{rr}) \\
& X_{rr}(t = 0) = \frac{R_e X_{exit} + X_{P7}}{R_e + 1} \\
& X_{exit} = \sum_i \sum_j f_r(i,j)\, X_{rr}(i,j) \qquad \text{(P8)} \\
& \sum_i \sum_j \lambda_{ij} = 1.0 \\
& \sum_i \sum_j f_r(i,j) = 1.0 \\
& \tau_R < \tau_{max} \\
& l \le X_{exit} \le u
\end{aligned}
$$

Here, J_{rr} is the value of the objective function at the exit of the recycle reactor; J_{P7} is the value of the objective obtained from the solution of (P7). λ_{ij} is the convex combiner of all points available from the CFR model. The variables X_{rr} and R_e represent the concentrations in the recycle reactor extension and the recycle ratio, respectively. X_{exit} is the vector of exit concentrations from the RR reactor. f_r is a linear combiner of all the concentrations from the plug flow section of the recycle reactor.

The next iteration consists of creating the new convex hull of concentrations, which include the concentrations obtained by this extension, and checking for favorable recycle reactor extensions from this new convex hull. At iteration P, this involves the solution of the following nonlinear programming problem:

$$
\begin{aligned}
\underset{R_e, \lambda_{ij},\ f_{\text{model}(p)}, T_{rr}(t)}{\text{Max}} \quad & J^{(P+1)}(v) \\
& \frac{dX_{rr}}{dt} = R(X_{rr},\ T_{rr}(t)) \\
& X_{rr}\ (t = 0) = \frac{R_e\, X_{\text{exit}} + X_{\text{update}}}{R_e + 1} \\
& X_{\text{update}} = \sum_i \sum_j \lambda_{ij}\, X_{cf}(i,j) + \sum_{p=1}^{P} f_{\text{model}(p)}\, X_{\text{model}(p)} \\
& X_{\text{exit}} = \sum_i \sum_j f_r(i,j)\, X_{rr}(i,j) \\
& \sum_i \sum_j \lambda_{ij} + \sum_{p=1}^{P} f_{\text{model}(p)} = 1.0
\end{aligned}
\tag{P9}
$$

Here, $X_{\text{model}(p)}$ is a constant vector and reflects the concentration at the exit at iteration p in the models previously chosen. A convex combination of this with the cross-flow region described by (P7) gives the fresh feed point for the recycle reactor we are looking for, X_{update}. X_{exit} then represents the concentration at the exit of the recycle reactor; and if $J^{(P+1)} > J^{(P)}$, the earlier model chosen is insufficient. The control profiles are $[f, f_{\text{model}(p)}]$ and T_{rr}, which are the linear combiners used to provide a convex candidate and the temperature profile in the recycle reactor, respectively. This procedure is repeated until no improvement in the objective function is observed. Figure 8 illustrates the flowchart for the synthesis procedure.

It is easy to see that with this approach, the reactor network is synthesized readily. Also, because of its stagewise nature, only the simplest reactor model needed is solved. In fact, for many problems, the solution is obtained through just one iteration of the flowchart in Fig. 8, mainly because the variable tem-

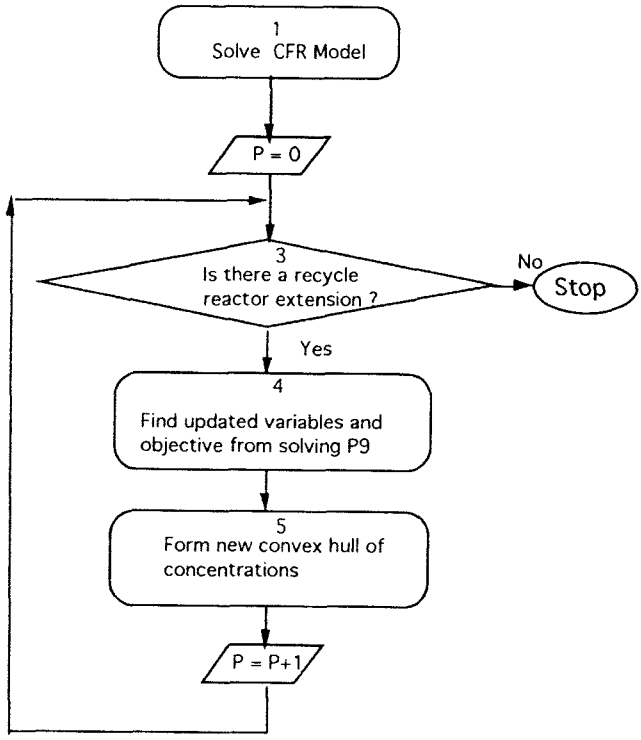

FIG. 8. Flowchart for reactor synthesis.

perature profile allows such a large area for the AR. It can be shown that this algorithm will converge to the optimal solution as long as *nonmonotonic* extensions to the AR are not encountered (as in Example 3). The examples solved in Balakrishna and Biegler (1992b), as well as the one shown next, suggest that this restriction does not seem to be limiting for the applicability of the proposed approach.

Example 5: Here, we maximize the conversion in the catalytic oxidation of sulfur dioxide in fixed-bed reactors, which has been investigated by Lee and Aris (1963). The reaction and the kinetics are described as follows:

$$SO_2 + {}^1/_2O_2 = SO_3$$

$$R(g,t) = 3.6 \times 10^6 \left[\exp\left\{12.07 - \frac{50}{1 + 0.311t}\right\} \frac{\{2.5 - g\}^{0.5}\{3.46 - 0.5g\}}{\{32.01 - 0.5g\}^{1.5}} - \exp\left\{22.75 - \frac{86.45}{1 + 0.311t}\right\} \frac{g\{3.46 - 0.5g\}^{0.5}}{\{32.01 - 0.5g\}\{2.5 - g\}^{0.5}}\right]$$

where g is defined as the number of moles of SO_3 formed per unit mass of mixture and t is defined as $(T - T_0)/J$, where T is the temperature, T_0 is 310 K (fresh feed temperature), and $J = 96.5$ K kg mol^{-1}. $R(g, t)$, the rate of reaction is defined as the kilogram-moles of SO_3 produced per hour per kilogram of catalyst. The extent of reaction, or the moles of SO_3 formed per unit mass of mixture, is limited by the inlet mass flow of SO_2, which is fixed at 2.5 mol SO_2 per unit mass of mixture. Lee and Aris looked at the maximization of an objective function based on the value of the product stream, catalyst, and preheating costs. However, they assumed adiabatic reactor sections, with cold-shot cooling. In our procedure, we do not enforce the adiabatic restriction, choosing yield maximization as our objective instead.

For this reaction, we observed that for a constraint on residence time of 0.25 s, the maximum reaction extent of 2.42 is obtained in a PFR with the temperature profile shown in Fig. 9a. The resulting optimization problem (555

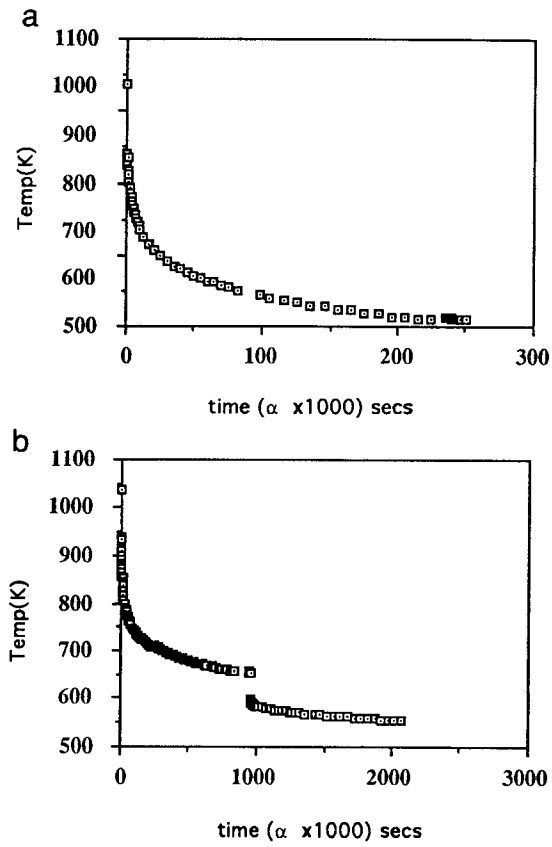

FIG. 9. Temperature profile for Lee–Aris example: (a) Residence time = 0.25 s; (b) large residence times.

equations, 753 variables) took 1503 CPU seconds on a VAX 3200 workstation. However, if the constraint on the residence time is removed, the extent of reaction (as defined by g) asymptotically approaches the upper bound of 2.5 in a PFR with a sufficiently large residence time. Also, for a residence time bound of 2.2 s, the temperature profile as a function of time is shown in Fig. 9b and delivers an extent of reaction of 2.48. Additional nonisothermal examples are considered in Balakrishna and Biegler (1992b).

V. Energy Integration of Reactor Networks

Energy integration involves the matching of heat loads between a set of hot streams and cold streams to minimize the cost of utilities for the network. Algorithms for the "isolated" construction of heat-exchanger networks (HENs) are well known. However, the synergy among process subsystems is a key area for the exploitation of energy integration. Reactor networks, in particular, are associated with significant heat effects and strongly influence the behavior of other subsystems. In this section, we address integration of the heat effects within the reactor with the rest of the process and demonstrate the effectiveness of the optimization formulations of the previous section.

Often, the reactor is the most important unit of the chemical plant because the downstream processing steps and the feed processing steps depend on the selective conversion of raw material into product. Here, the difference between stand-alone reactor network synthesis and reactor-flowsheet integration is that the constraints within the flowsheet allow a variable, but usually bounded, space of inlet concentrations for the reactor. If the space of inlet concentrations is not predetermined, then the problem size increases at each iteration of the constructive approach. This is because the previous reactors (or previous convex hulls) are not fixed, at each iteration, owing to the infinite number of inlet concentrations dictated by the flowsheet constraints. Nevertheless, the optimization formulations developed in the previous two sections can be readily adapted to determine the optimal flowsheet parameters. The development of a model for the energy integration of reactors is presented next. Following this, we apply our formulations to generate reactor extensions and illustrate this approach for the design of energy-integrated, reactor-based flowsheets.

A. Model Formulation for Energy Integration

We consider two approaches for the integration of the reactor and energy network: the *sequential* and the *simultaneous* formulations. In the conventional

sequential approach, the reactor and separator schemes appear at a level higher relative to energy integration. In other words, once the "optimal" flowsheet parameters have been determined for the reactor target and the separation system, the reactor network is realized, and the heat-exchanger network is derived in a straightforward manner. However, it is well known that this approach can be suboptimal with respect to the overall flowsheet (Duran and Grossmann, 1986).

For the simultaneous approach, we consider reactor synthesis and energy integration at the same level. This approach is attractive because it considers the strong interaction between the chemical process and the heat-exchanger network. However, this is not a trivial problem because the flowrates and the temperature of the process streams are not known in advance. Moreover, we do not restrict ourselves to adiabatic or isothermal constraints on the temperature profile within the reactor. Therefore, the streams within the reactor cannot be classified as hot or cold streams *a priori,* because the nature of the optimal temperature trajectory within the reactor is unknown. Instead, we discretize the temperature trajectory in the CFR model proposed for nonisothermal reactor synthesis, and introduce the concept of candidate streams within the reactor network. Here, we approximate the optimal temperature trajectory within the reactor by a set of isothermal segments followed by the temperature change between these segments as shown in Fig. 10. The solid curve represents the actual trajectory, while horizontal lines represent isothermal reacting segments and vertical lines represent the temperature changes necessary to follow an optimal trajectory.

The horizontal segments at constant temperature correspond either to hot streams or cold streams, depending on whether the reaction is exothermic or endothermic, while the vertical sections involve heating or cooling; therefore we assume the presence of both heaters and coolers between the reacting segments. Also, we call these hot or cold streams *candidate* streams, because they

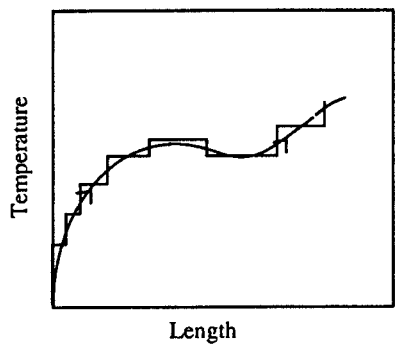

FIG. 10. Piecewise constant approximation of optimal reactor temperature profiles.

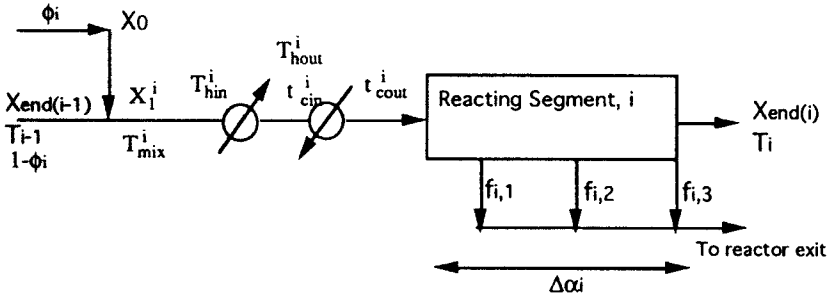

FIG. 11. Reacting segment for heat integration.

may or may not be present in the optimal network. This will depend on the exit flow distribution, which may include only some of the reacting segments and hence the corresponding temperature profiles. The schematic in Fig. 11 shows the reactor representation (of the CFR model for nonisothermal networks) corresponding to the above approximation.

The representation in Fig. 11 is similar to the discretized representation of the cross-flow reactor shown in Fig. 7, except for the additional heat exchangers. The subscript i again represents the ith finite element corresponding to the discretization. T^i_{mix} corresponds to the temperature after mixing the reacting stream with the feed. T^i_{hin}, T^i_{hout} correspond to the temperatures of the streams entering and leaving the heater, and t^i_{cin}, t^i_{cout} correspond to the temperatures of the streams entering and leaving the cooler. In an optimal network, it can be shown that only one of these two heat exchangers will be chosen. $\Delta\alpha_i$ corresponds to the length of the finite element, which may also be a variable in the optimization problem (subject to constraints on error control). Thus, the problem is well posed since we now know the hot and cold streams *a priori*, even if the flow rates and the temperatures are not known. Also, some amount of temperature control can be achieved by mixing, while the remainder can be accomplished by the utilities or the heat flows within the network. Using the framework for reactor targeting from above, we now integrate this within a suitable energy targeting framework. We assume here that utility costs will predominate and will be sufficient for the simultaneous total flowsheet synthesis for preliminary design. However, overall capital cost and area estimates for the heat-exchanger networks (Kravanja and Grossmann, 1990) can also be included here if desired.

Duran and Grossmann (1986) derived analytical expressions for minimum utility consumption as a function of flowrates and temperatures of the heat-exchange streams. They showed that given a set of hot and cold streams, the minimum heating utility consumption is given by $Q_H = \max(z_H^P)$, where

z_H^p is the difference between the heat sources and sinks above the pinch point for pinch candidate p. For hot and cold streams with inlet temperatures given by T_h^{in} and t_c^{in}; and outlet temperatures T_h^{out} and t_c^{out} respectively, z_H^p (y) is given by

$$z_H^p(y) = \sum_{c \in C} w_c[\max\{0; t_c^{out} - \{T^p - \Delta T_m\}\} - \max\{0; t_c^{in} - \{T^p - \Delta T_m\}\}]$$

$$- \sum_{h \in H} W_h[\max\{0; T_h^{in} - T^p\} - \max\{0; T_h^{out} - T^p\}]$$

for $p = 1, ..., N_p$; where N_p is the total number of heat-exchange streams. Here, T^p corresponds to all the candidate pinch points; these are given by the inlet temperatures for all hot streams and the inlet temperature added to ΔT_m for the cold streams. w_c and W_h are the heat capacity flows for the hot and cold streams. Also, y is the set of all variables in the reactor and energy network. The minimum cooling utility is given by a simple energy balance as $Q_C = Q_H + \Omega(y)$; where, $\Omega(y)$ is the difference in the heat content between the hot and the cold process streams, given by:

$$\Omega(y) = \sum_h W_h(T_h^{in} - T_h^{out}) - \sum_c w_c(t_c^{out} - t_c^{in})$$

Based on the above concepts for reactor and energy network synthesis, a unified target for simultaneous reactor-energy synthesis can now be formulated. We first classify the streams within the process into four categories. Let H_R, C_R be the set of hot and cold streams associated with the reactor network and let H_P, C_P be the set of hot and cold streams in the process flowsheet. Also, $h \in H = H_R \cup H_P$, and $c \in C = C_R \cup C_P$. If there are NE isothermal reacting segments and if the reaction is exothermic, then there is a set of NE hot reacting streams from which the heat of reaction is to be removed in order to maintain a desired temperature in each segment. Also, between any two elements, there is a hot stream corresponding to the discretization shown in Fig. 11. Hence, H_R is a set of cardinality 2NE, while C_R is a set of cardinality NE. For an endothermic reaction, C_R and H_R have cardinalities in the reverse order, since the reacting segments now correspond to cold streams. Thus, there are always 3NE candidate streams, some of which may have zero heat content in the reactor network. Let F_h and F_c denote the mass flow rates of the hot and cold streams respectively. $F_{(i)}$ denotes the mass flow at the entry point of reacting segment i, F_0 is the total inlet flow into the reactor, heat capacities are allowed to be temperature-dependent. In addition, ω constitutes the variables in the flowsheet. Based on these assumptions, a unified target for simultaneous reactor-energy synthesis can be obtained by extending (P7) to include the Duran and Gross-

mann heat integration model for the reactor network and flowsheet. This requires the solution of the following nonlinear programming problem:

$$
\begin{aligned}
\text{Max} \quad & \Phi(\omega,y,Q_H, Q_C) = J(\omega,y) - c_H Q_H - c_C Q_C \\
\text{s.t.} \quad & \sum_k X_{ik} L_k'(\alpha_j) - R(X_{ij}, T_{ij}) \Delta\alpha_i = 0 \qquad j = 1, K \\
& X(0) = X_0(\omega,y) \\
& X_{i\text{end}} = \sum_k X_{ik} L_k(t_{\text{end}}) \\
& X_{i,0} = \phi_i X_0 + (1 - \phi_i) X_{(i-1)\text{end}} \\
& X_{\text{exit}} = \sum_i \sum_j X_{ij} f_{ij} \\
& \sum_{ij} (f_{ij} - q_{ij}) \alpha_{ij} = \tau \\
& \sum_{ij} f_{ij} = 1 \\
& F_{(0)} = \phi_0 F_0 \\
& F_{(ij)} = \sum_i \phi_i F_{(i,0)} - \sum_{ij} f_{ij} F_0 \\
& Q_C = Q_H + \sum_{h \in H} W_h [T_h^{\text{in}} - T_h^{\text{out}}] - \sum_{c \in C} w_c [t_c^{\text{out}} - t_c^{\text{in}}] \\
& Q_H \geq z_H^P(y) \\
& h(\omega,y) = 0 \\
& g(\omega,y) \leq 0
\end{aligned}
\tag{P10}
$$

Here, T^P corresponds to all the inlet temperatures for the hot streams, and $t_c^{\text{in}} + \Delta T_m$ denotes all the cold streams. The heats of reaction are directly accounted for by the heat capacity flow rates of the reacting streams as follows. If Q_R is the heat of reaction to be removed (or added, for endothermic reactions) to maintain an isothermal reacting segment, the equivalent $(FC_p)_h$ or W_h for this reacting stream is equated to Q_R, and we assume a 1 K temperature difference for this reacting stream. In addition, the relations involving $h(\omega,y)$ and $g(\omega,y)$ are derived from interactions due to the rest of the flowsheet.

Finally, the max(0, Z) functions, which make up the $z_H^P(y)$ relations, have a nondifferentiability at the origin, which can lead to failure of the NLP solver. In order to provide smooth problem formulations, we approximate max(0, Z) as

$$f(Z) = \max(0, Z) \approx \frac{\text{sqrt}(Z^2 + \epsilon^2)}{2} + \frac{Z}{2}$$

With values of $\epsilon = 0.01$, we were able to obtain a reasonably good approximation to the max function while simultaneously allowing easier solution of problem (P10). The advantage in this representation is that it provides a single function approximation over the entire domain.

B. Extensions from the Targeting Model

The solution of the nonlinear optimization problem (P10) gives us a lower bound on the objective function for the flowsheet. However, the cross-flow model may not be sufficient for the network, and we need to check for reactor extensions that improve our objective function beyond those available from the cross-flow reactor. We have already considered nonisothermal systems in the previous section. However, for simultaneous reactor energy synthesis, the dimensionality of the problem increases with each iteration of the algorithm in Fig. 8 because the heat effects in the reactor affect the heat integration of the process streams. Here, we check for CSTR extensions from the convex hull of the cross-flow reactor model, in much the same spirit as the illustration in Fig. 5, except that all the flowsheet constraints are included in each iteration. A CSTR extension to the convex hull of the cross-flow reactor constitutes the addition of the following terms to (P10) in order to maximize $\Phi(2)$ instead of Φ:

$$\begin{aligned} \text{Max} \quad & \Phi^{(2)}(\omega, y^{(2)}, Q_H, Q_C) = J(\omega, y^{(2)}) - c_H Q_H - c_C Q_C \\ \text{s.t.} \quad & X_{cstr} = X_{exit} + R(X_{cstr}, T_{cstr})\, \tau_{cstr} \\ & \tau \geq 0, \qquad X_{cstr} \geq 0 \end{aligned} \tag{P11}$$

Here, X_{cstr} corresponds to the new reactor extension and $y^{(2)}$ is the set of new variables in the reactor and energy network. Besides the variables ω and y in (P10), this includes the variables corresponding to the new CSTR extension, namely, X_{cstr}, T_{cstr}, τ_{cstr}, and three more candidate streams for heat exchange. This is because the two heat exchangers will either cool or heat the feed to the CSTR (only one of these will exist in the optimal network), and one additional exchanger within the CSTR will maintain a desired temperature. If $\Phi^{(2)*} > \Phi^*$, we have a reactor extension that improves the objective function. The next step consists of creating the new convex hull of concentrations and checking for extensions that improve our objective function within the flowsheet constraints. As in Sections III and IV, we continue this procedure until there are no extensions that improve the objective function.

C. Energy-Integration Example

We now provide a small process example to illustrate the simultaneous synthesis of reactor and energy networks. Here, we consider a reaction mechanism in the van de Vusse form, though with kinetic expressions different from those used above. The integrated flowsheet corresponding to the synthesis problem is shown in Fig. 12.

The feed to the plant consists of pure A. This is mixed with the recycle gas stream consisting of almost pure A, and preheated (C1) before entering the reactor. After reaction, the mixture of A, B, C, and D passes through an aftercooler prior to distillation. In the first column, A is recovered and recycled, while in the second column, the desired product B is separated from CD, which is used as fuel. The distillation columns are assumed to operate with a constant temperature difference between reboiler and condenser temperatures (Andrecovich and Westerberg, 1985). The reflux ratios are fixed and the column temperatures are functions of the pressure in the column, which is variable so that efficient heat integration can be attained between the distillation columns and the rest of the process. The reactions involved in this flowsheet are as follows:

$$\begin{array}{ccccc} A & \xrightarrow{k_1} & B & \xrightarrow{k_2} & C \\ {\scriptstyle k_3}\downarrow & & & & \\ D & & & & \end{array}$$

where $k_{10} = 8.86 \times 10^6\ h^{-1}$, $k_{20} = 9.7 \times 10^9\ h^{-1}$, $k_{30} = 9.83 \times 10^3$ liters $mol^{-1}\ h^{-1}$; $E_1 = 15.00$ kcal/g-mol, $E_2 = 22.70$ kcal/g-mol, and $E_3 = 6.920$ kcal/g-mol; and $\Delta H_{A\to B} = -0.4802$ kcal/g-mol, $\Delta H_{B\to C} = -0.918$ kcal/g-mol, and $\Delta H_{A\to D} = -0.792$ kcal/g-mol of A.

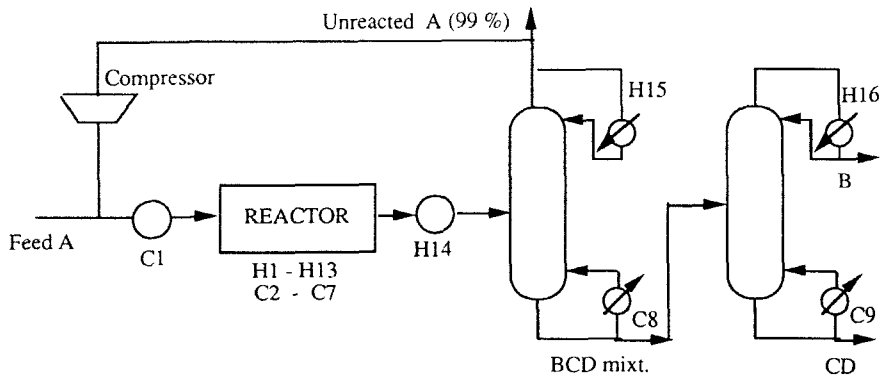

Fig. 12. Flowsheet for reactor–energy network synthesis.

The reactor is represented by the cross-flow discretization shown in Fig. 11. Here, we choose seven reactor segments (NE=7), with uniform segment lengths, $\Delta\alpha_i$. Since the reaction is exothermic, this corresponds to 14 hot streams and 7 cold streams. Thus, the streams in the reactor may be enumerated as hot streams H1–H13 (2NE − 1, since the entry point is fixed to be a preheater), and cold streams C1–C7. The streams H15–H16, and C8–C9 correspond to the condensers and reboilers of the distillation column. As described in (P10), the specific heats are assumed to be linear with the inlet temperatures. The objective function here as the total profit for the plant and is given in simplified form by

$$J = 1.7F_B + 0.8F_{CD} - 6.95 \times 10^{-5}\tau F_0 - 0.4566F_B(1 + 0.01(T_{H15}^{in} - 320))$$
$$- 0.7(F_B + F_{CD}) - 0.2F_{A0} - 0.007Q_C - 0.08Q_H$$

Further details of this formulation can be found in Balakrishna and Biegler (1992b). In this expression, F_B and F_{CD} represent the production rates of B and CD, respectively. F_{A0} is the flow rate of fresh feed. The third term corresponds to the reactor capital cost with τ, the residence time, and F_0, the total reactor feed; the fourth and the fifth terms correspond to the capital cost of the distillation columns. The operating costs of the columns are directly incorporated into the energy network in terms of condenser and reboiler heat loads. We assume that the cost of the reactor can be described by the total residence time and is independent of the type of reactor. The potential error from this assumption can be justified because the capital cost of the reactor itself is usually an order of magnitude or more smaller than the operating costs and the capital costs of the downstream processing steps.

Here, we consider two alternatives. First, we consider the sequential approach, where we optimize the reactor network with an optimal temperature profile, then integrate the maintenance of this optimal profile with the energy flows in the rest of the flowsheet. In the second case, we solve the above problem with the simultaneous formulation proposed in (P10).

The optimization model in the sequential case had 342 equations and 362 variables for the reactor flowsheet optimization (96 CPU seconds on the VAX 6320) and 200 equations and 161 variables for the energy integration (170 CPU seconds). The simultaneous optimization model (542 equations, 523 variables) was solved in 1455 CPU seconds and was initialized with the solution to the sequential model. Table I presents a comparison between the results for sequential and simultaneous modes to synthesis. A target production rate of 40,000 lb/h is assumed for the desired product B.

Clearly, the simultaneous formulation leads to a significant improvement in the overall profit and conversion due to the correct anticipation of the energy costs in the reactor design. Even though the shape of the temperature profiles is not markedly different, the temperatures in the simultaneous case are lower,

TABLE I
COMPARISON BETWEEN SEQUENTIAL AND SIMULTANEOUS FORMULATIONS

	Sequential	Simultaneous
Overall profit	38.98×10^5 \$/year	74.02×10^5 \$/year
Overall conversion	49.6%	61.55%
Hot utility load	3.101×10^5 BTU/h	2.801×10^5 BTU/h
Cold utility load	252.2×10^6 BTU/h	168.5×10^6 BTU/h
Fresh feed A	8.057×10^4 lb/h	6.466×10^4 lb/h
Degraded product C	3.112×10^4 lb/h	1.44×10^4 lb/h
By-product D	0.933×10^4 lb/h	1.00×10^4 lb/h
Unreacted (recycled) A	1.22×10^4 lb/h	1.963×10^4 lb/h

as seen in Fig. 13. These lower temperatures lead to a significant reduction in the degradation of product B to by-product C, as seen in Table I. Since the B–C reaction is also the most exothermic, the retardation of this reaction leads to less heat evolution and therefore less cold utility consumption. Furthermore, the more efficient conversion to B results in less consumption of raw material A, leading to higher overall conversion and less total flow within the reactor in the simultaneous case. This results in lower heat capacity flow rates for the reacting hot streams, and hence lower cold utility consumption. However, the optimal reactor in both sequential and simultaneous cases (a nonisothermal PFR) has the same residence time of 0.59 s. Since the temperatures are lower in the simultaneous case, the conversion per pass of A is actually lower in the simultaneous case, leading to higher recycles in the simultaneous case. In either case, of the 20 candidate streams, only 12 streams are active in the optimal network. This is because the strictly falling temperature profiles avoid the use of any cold streams (C2–C7) within the reactor network.

In addition, no mixing was predicted in the solution, so cold-shot cooling was not used at all. However, this decision is directly influenced by the ratio of the raw material to energy costs. For small ratios, even if mixing is not optimal in concentration space, the energy costs may drive the use of cold shots in order to reduce utility consumption. Within the constraints on the residence time ($\tau^{up}=$

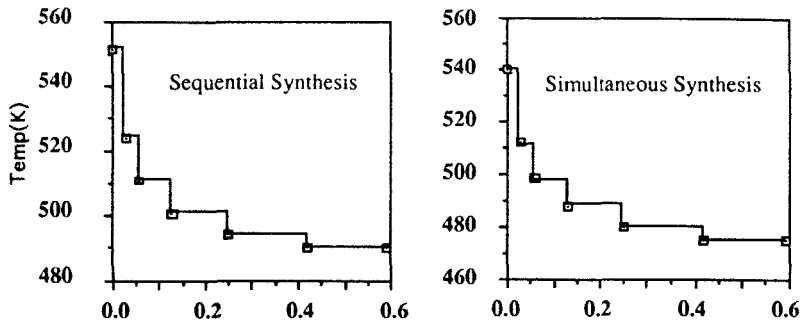

FIG. 13. Reactor temperature profiles.

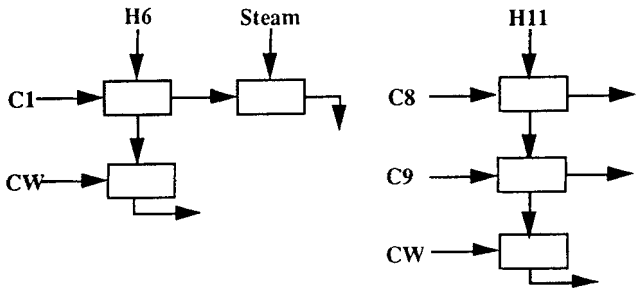

FIG. 14. Heat-exchanger network substructure.

1.00 s), no further extensions that improve the objective function are found from these solutions to either the sequential or the simultaneous targeting model. The pinch points correspond to 546.5 K and 535.1 K for the sequential and simultaneous schemes, respectively. Also, the heat loads for the hot streams are significantly higher than those for the cold streams. Thus, the cooling (or T–Q curves) for the hot streams will be nearly flat. Since the pinch corresponds to the inlet temperature of the hottest hot stream in either case, no part of the T–Q curve for the hot streams will extend beyond the pinch. The matches below the pinch are thus very easily determined. In fact, streams C1, C8, and C9 can be matched with any of the streams from H1 to H11, without any alteration in the utility cost. The network in this case is thus innately flexible; the primary reason for this is the significant disparity in the heat contents due to the high reaction exothermicity.

One feasible network would correspond to the cold streams C1, C8, and C9 diverted to suitable jacketed reactor compartments, as the simple network in Fig. 14 shows. The hot streams not shown in this network are matched directly with cooling water (CW), and the amount of steam used here is very small. Note that this network would require the same minimum utility consumption predicted by the solution of (P10). It can be inferred that the network in Fig. 14 is equally suitable for both the simultaneous and sequential solutions. In fact, Balakrishna and Biegler (1993) showed that, for exothermic systems in which the reactor temperature is the highest process temperature, the pinch point is known *a priori* as the highest reactor temperature (in this case, the feed temperature) and the inequality constraints in (P10), $Q_H \geq z_H^p(y)$, $p \in P$, can be replaced by a simple energy balance constraint. This greatly reduces the computational effort to solve (P10).

VI. Simultaneous Reaction, Separation, and Energy System Synthesis

Previous studies on process integration have generally considered reaction and separation as processes that occur sequentially in a flowsheet. In this section,

a unified formalism is presented for the synthesis of reaction–separation systems while ensuring optimal energy management. The synthesis approach is developed in the light of the ideas previously presented on the sequential bounding scheme for reactor targeting. While previous formulations have considered reaction and separation as sequential operations in a flowsheet, our model is developed to consider simultaneous reaction and separation as an option within the network. Such simultaneous events occur, for example, in reactive distillation and membrane reactors.

We first develop a nonisothermal reactor model, which allows for separation as reaction progresses. This is facilitated through a species-dependent residence time distribution. Optimization of this residence time distribution function leads to a separation profile as a function of age. The synthesis model is then formulated as a mixed-integer optimal control problem, where the integer variables account for the fixed costs of separation. The control profiles include the temperature, the separation profile, and some mixing functions defined for the network. Costs for maintaining a separation profile are addressed next by defining a separation index (defined to model the intensity of separation) and a fixed charge for any separation between two components in the reaction mixture. Following this, we consider the amalgamation of this formulation with energy minimization and develop simplifications for systems with highly exothermic reactions. The solution to this model gives us a lower bound on the performance index; we therefore present schemes to successively improve these bounds, based on reactor extensions.

A. Combined Reaction–Separation Model

Figure 15 gives a schematic of a simultaneous reaction–separation model. To include separation in a reactor targeting model, we postulate a separation function vector (γ) analogous to a residence time distribution function for homogeneous reactors. Here, however, each species has its own residence time distribution function, which is dependent on its separation function γ_c.

If we define $m_c(\alpha)$ as the mass of component c (c = 1, ..., C) at time α, then a mass balance around the network in Fig. 15 leads to

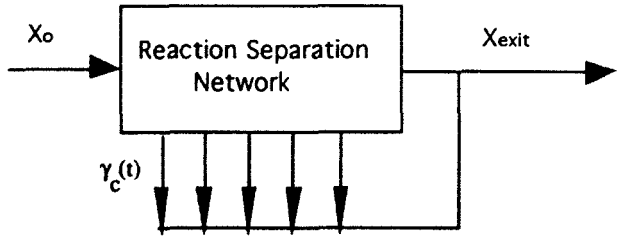

Fig. 15. Flow model for combined reaction–separation targeting.

$$\frac{d\sum_{c=1}^{C} m}{d\alpha} = -\sum_{c=1}^{C} \gamma_c(\alpha) m_c(\alpha)$$

where $\gamma_c(\alpha)$ is a continuous function of α. For a homogenous system, if ρ is the density of the system, then

$$\frac{dQ}{d\alpha} = -\sum_{c=1}^{C} \frac{\gamma_c(\alpha) m_c(\alpha)}{\rho}$$

We assume constant-density systems for the sake of simplicity, even though variable density could be considered by a straightforward extension of this model.

Now a differential balance around an infinitesimal element of α for component c gives

$$\frac{dX_c}{d\alpha} = R_c(X,T) + X_c(\alpha)\left[\frac{\gamma(\alpha)^T X(\alpha)}{\rho} - \gamma_c(\alpha)\right]$$

With this governing equation, a mathematical model for maximizing the performance index in this reacting environment can be derived as follows:

$$\begin{aligned}
\underset{\gamma,T}{\text{Max}} \quad & J_{\text{exit}}(m_{c(\text{exit})}, Q, \tau) \\
& \frac{dX_c}{d\alpha} = R_c(X,T) + X_c(\alpha)\left[\frac{\gamma(\alpha)^T X(\alpha)}{\rho} - \gamma_c(\alpha)\right]; \qquad c = 1, C \\
& \frac{dQ}{d\alpha} = -\sum_{c=1}^{C} \frac{\gamma_c(\alpha) m_c(\alpha)}{\rho} \\
& m(\alpha) = X(\alpha) Q(\alpha) \\
& m_c(0) = m_{c0} \\
& \sum_{c=1}^{C} m_c(0) = \sum_{c=1}^{C} m_c(\text{exit}) \\
& m_c(\text{exit}) = \int_0^\infty \gamma_c(\alpha) m_c(\alpha)\, d\alpha \\
& \tau = \int_0^\infty \alpha f(\alpha)\, d\alpha \\
& g(\gamma, X, \mu) \le 0 \\
& h(\gamma, X, \mu) = 0
\end{aligned} \tag{P12}$$

Here, J is an objective function specified by the designer, $X(\alpha)$ is the mass concentration vector of molecules of age α, m_{c0} is the mass flow of each species

at the entrance to the reactor, and m_c(exit) is the mass flow of each species at the reactor exit given as the integral of outlet flows at different points within the reacting system. The residence time, τ, is determined from the RTD function $f(\alpha)$. Also, g and h represent the inequality and equality constraints imposed by the process variables (μ) on the reaction system.

Clearly, formulation (P12) is an optimal control problem with differential equation constraints, where the γ_c's, and the temperature are the control profiles. The solution to this model will give us the optimal separation profile along the reactor. It is clear that $\gamma(\alpha)$ models the effect of separation within the reactor network. If all the elements of the vector $\gamma(\alpha)$ are the same (which implies that there is no relative separation between the species in the reactor), the second term for the governing differential equation vanishes, since

$$\gamma(\alpha)^T X(\alpha) = \sum_{c=1}^{C} \gamma_c X_c = \gamma_c \sum_{c=1}^{C} X_c = \gamma_c \rho$$

therefore

$$\left[\frac{\gamma(\alpha)^T X(\alpha)}{\rho} - \gamma_c(\alpha)\right] = 0; \qquad \forall\, c \in C$$

Thus, the governing equation to this reactor scheme reduces to that of segregated flow, and the formulation reduces to the segregated flow optimization problem in Section III. Furthermore, the γ_c's can now be directly related to the RTD function (Balakrishna and Biegler, 1993) through the following relation:

$$\gamma_c(\alpha) = \frac{f(\alpha)}{1 - F(\alpha)}$$

where f(α) is the true residence time distribution of the molecules within the reactor network, and F(α) is the cumulative RTD = $\int_0^\alpha f(t)\, dt$.

However, if the γ_c's are not the same for all components—i.e, there exists a separation profile—then the actual RTD for this system is given by:

$$f(\alpha) = \sum_c \frac{\gamma_c(\alpha) q_c(\alpha)}{Q_0}$$

where $q_c(\alpha) = m_c(\alpha)/\rho$.

The solution to (P12) gives us the optimal separation profile as a function of age within the reactor. However, except in the case of reactive phase equilibrium, the assumption of a continuous separation profile is not really required. Furthermore, a continuous separation profile may not be implementable in practice. To address this, we take advantage of the structure of a discretization procedure for the differential equation system. In this case, we choose orthogonal collocation on finite elements to discretize the above model. This results

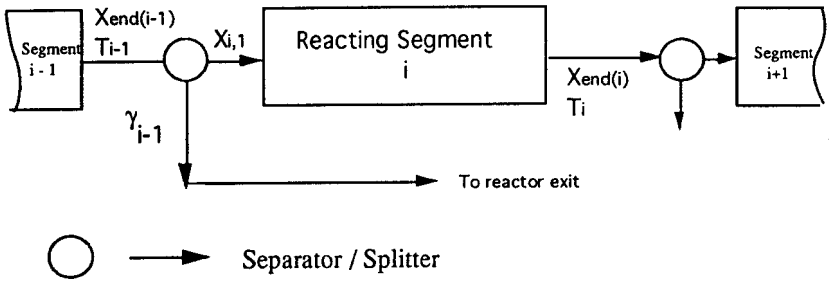

FIG. 16. Finite-element discretization for reaction–separation targeting model.

in a reactor structure as shown in Fig. 16, where we restrict separation only to the ends of each finite element. Also, the differential equations are now converted to algebraic equations through collocation, and the optimal control problem is reduced to the nonlinear program shown in (P13). Furthermore, it can be shown that as $\Delta\alpha$ tends to zero, this discretized model is equivalent to the original optimal control problem. [A proof for this equivalence can be found in Balakrishna and Biegler (1993).] The $\gamma_c(\alpha)$ in the original model now reduces to a mass split fraction vector of each species at the end of each element ($\gamma_{c,i}$). Finally, the control profiles, temperature (T), separation fractions (γ_c), and the RTD are assumed to be piecewise constant over each element.

$$
\begin{aligned}
\underset{\gamma,T}{\text{Max}} \quad & J_{\text{exit}}(m_{\text{exit}}, Q, \tau) \\
& \sum_k X_{ik}\, L_k'(t_j)/\Delta\alpha_i - R(X_{ij}, T_{ij}) = 0 \qquad @\ t_j \quad \text{s.t. } j \neq 0 \\
& X(0) = X_0 \\
& X_{i\text{end}} = \sum_k X_{ik}\, L_k(t_{\text{end}}) \\
& m_{c,i+1} = [X_{c,i\text{end}}]\, Q_i\, [1 - \gamma_{c,i}] \\
& X_{i1}\, Q_{(i)} = m_i \qquad \text{(P13)} \\
& Q_{(i+1)} = Q_i \left[1 - \sum_{c=1}^{C} X_{c,i\text{end}}\, \gamma_{c,i}/\rho\right] \\
& m_{c,\text{exit}} = \sum_i X_{c,i\text{end}}\, \gamma_{c,i}\, Q_i \\
& f(i) = \sum_{c=1}^{C} \gamma_{c,i}\, m_{c,i}/Q_0 \\
& \tau = \sum_i f(i)\, t(i) \leq t_{\max} \\
& \sum_i \Delta\alpha_i = t_{\max}
\end{aligned}
$$

where

X_{ij} = Mass concentration vector at collocation point j in finite element i (point $[i,j]$)
$L_k'(t_j)$ = Derivative of Lagrange interpolation polynomial at $[i,j]$
γ_i = Mass split fraction vector at the end of finite element i (array of $\gamma_{c,i}$)
$f(i)$ = Actual RTD for the system at element i
T_{ij} = Temperature at $[i,j]$
$X_{i\text{end}}$ = Mass concentration vector at the end of element i.
m_i = Species mass flow vector entering element i
Q_i = Total volumetric flow rate entering element i

The first three constraints represent orthogonal collocation applied to the differential equations at the collocation points. The next three equations represent mass balances at the separation point. The discretized RTD function and the expression for the mean residence time are given in the final constraints. As $\Delta\alpha \rightarrow 0$, this model is equivalent to the original reaction–separation model (P12). The main difference is that we allow separation only at the end of each element; within each element no separation occurs. Although the model appears nonlinear, the nonlinearities are actually reduced when one considers the rates in terms of the mass fractions. The solution to this model then gives us the optimal separation split fractions as a function of time along the reactor.

One important issue that still needs attention is the objective function. It is intuitively obvious that if a separation cost is not associated with it, we will usually end up getting near-complete separations of products, and hence complete conversions to the extent possible within stoichiometric constraints. Thus the AR in concentration space can easily be the entire stoichiometric space. Unfortunately, it is difficult to get an accurate representation for the separation cost, especially when sharp splits are not enforced. Here, we present a simple cost model by assuming that the variable cost of separation is determined by two factors, namely, the difficulty of separation and the mass flow rate through the separator.

We first consider an example for modeling the separation costs. As shown in the schematic in Fig. 17, a stream with components A,B,C and mass flow rates F_A, F_B, F_C undergoes a separation operation into two output streams, with mass flow rates F_{A1}, F_{B1}, F_{C1} and mass flows F_{A2}, F_{B2}, F_{C2}, respectively. The streams A, B, and C are arranged in a sequential order of separability; for example, in the case of distillation, we may assume that A, B, and C are in decreasing order of volatility. The mass fractions γ_A, γ_B, and γ_C are then defined as

$$\gamma_A = F_{A1}/F_A, \qquad \gamma_B = F_{B1}/F_B, \qquad \gamma_C = F_{C1}/F_C$$

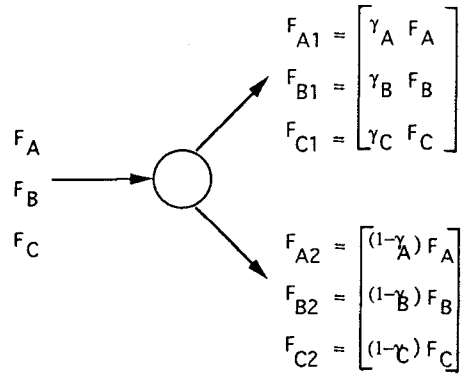

FIG. 17. Separation of mass fractions.

If the split fractions $\gamma_A = \gamma_B = \gamma_C$, we have only a splitting operation without any separation. Otherwise, there is a relative separation between two adjacent components in the mixture and we define $|\gamma_A - \gamma_B|$ as a measure of the intensity of separation between these two components. When $\gamma_A - \gamma_B = \gamma_B - \gamma_C = 0$, we have only a splitting operation among these components, and the cost of separation is identically zero; however, if $\gamma_A - \gamma_B = \pm 1$, we have a sharp split between components A and B. Any intermediate degree of separation could then be modeled by complete sharp split separation followed by mixing in order to achieve the desired composition.

We can generalize this to formulate the separation costs. Let $M = \{m\}$ denote the set of all components in the reacting system and let these be arranged in some monotonic order of relative separability, such as volatilities. If Q is the mass flow rate handled by the separator, the cost of separation may be described by

$$C_{\text{sep}} = C_{\text{capital}} + C_{\text{operating}}$$

$$C_{\text{capital}} = C_{\text{fixed}(mn)}\, y_{mn} + \sum_{m;n=m+1} p_{mn}\, |\Delta\gamma_{mn}| Q$$

Here, y_{mn} is the binary variable associated with the separation of components m and n, such that if $y_{mn} = 0$, then $\Delta\gamma_{mn} = 0$; and if $y_{mn} = 1$, then $\Delta\gamma_{mn} \leq 1$. The second term models the intensity of separation, where the cost coefficient p_{mn} for unit separation between two adjacent components m and n reflects the difficulty of separation between m and n. Q is the net flow through the separation network. The above formulation gives us an exact representation when we have sharp splits between adjacent components. As we mentioned earlier, nonsharp splits can be modeled by sharp splits followed by mixing, and an upper bound on the separation costs can be derived by enforcing $|\Delta\gamma_{mn}| = 1$ whenever $y_{mn} = 1$ (i.e., by assuming sharp splits) while a lower bound on the separation cost

is given by the expression above. The operating cost (reboiler and condenser duties in distillation, for example) can be directly incorporated into the energy minimization framework presented next.

The presence of $|\Delta\gamma_{mn}|$ in the cost function makes the objective function in (P13) nondifferentiable, so it is reformulated by adding the following terms within (P13):

$$\text{Max} \quad J_{\text{exit}} = J_{\text{product}}(m_{c(\text{exit})}, Q, \tau) - C_{\text{fixed}(mn)} y_{mn} - \sum_{m;n=m+1} p_{mn} \Delta_{mn} Q - C_{\text{operating}}$$

$$\Delta_{mn} \geq \gamma_m - \gamma_n$$

$$\Delta_{mn} \geq \gamma_n - \gamma_m$$

Since Δ_{mn} is to be minimized in the objective, it is easy to show that this reformulation would result in $\Delta_{mn} = |\Delta\gamma_{mn}|$, as desired, at the optimal solution.

This approach was applied to the Williams–Otto process (Balakrishna and Biegler, 1993). In previous studies, this process was optimized with a CSTR reactor followed by waste and product separators and a recycle stream. The application of (P12) to this problem led to a significantly improved process, particularly when the separation costs (p_{mn}) were low enough to allow coupled reaction and separation. Without separation, the optimal network is a single PFR with twice the return on investment of previous studies. Allowing for separation leads to a tubular reactor with sidestream separators to remove product and waste as they are created. The resulting process objective has a further fivefold improvement.

B. Unified Formulation for Optimal Energy Utilization

The combined reaction–separation model has advantages because it allows us to consider both reaction and separation within one framework. We now extend this formulation further to include energy minimization by using the concepts of pinch technology. Thus heat effects within the reactor and separator are integrated optimally with the energy flows in the flowsheet. The energy minimization scheme for this network closely follows the development in Section V, where our reactor targeting model was integrated with an energy targeting framework based on minimum utility consumption (Duran and Grossmann, 1986). The schematic in Fig. 18 shows one finite element of the discretized reactor–separator representation of Fig. 16 along with the candidate heat-exchange streams. Based on the development in Section V, a unified reactor–separator–energy target can be derived from the solution to the following mixed-integer nonlinear programming (MINLP) problem:

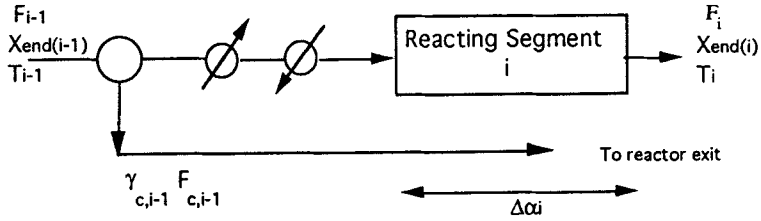

FIG. 18. Discretized model for energy minimization.

$$\text{Max} \quad \Gamma(\omega,\psi,Q_H,Q_C) = J(\omega,\psi) - c_H Q_H - c_C Q_C - C_{sep}$$

$$\text{s.t.} \quad \sum_k X_{ik} L_k'(\alpha_j) - R(X_{ij}, T_{ij})\Delta\alpha_i = 0 \qquad j = 1, K$$

$$X(0) = X_0$$

$$X_{iend} = \sum_k X_{ik} L_k(t_{end})$$

$$X_{c,i,0} F_i = (1 - \gamma_{c,i-1}) X_{c,(i-1)end} F_{(i-1)}$$

$$F_{c,exit} = \sum_i \gamma_{c,i} X_{c,(i)end} F_i$$

$$\Delta_{mn} \le y_{mn}$$

$$0 \le \gamma_i \le 1$$

$$\Delta_{mn} \ge \gamma_m - \gamma_n \qquad \text{(P14)}$$

$$\Delta_{mn} \ge \gamma_n - \gamma_m$$

$$Q_C = Q_H + \sum_{h\in H} W_h[T_h^{in} - T_h^{out}] - \sum_{c\in C} w_c[t_c^{out} - t_c^{in}]$$

$$z_H^P(\psi) = \sum_{c\in C} w_c[\max\{0; t_c^{out} - \{T^P - \Delta T_m\}\} - \max\{0; t_c^{in} - \{T^P - \Delta T_m\}\}] - \sum_{h\in H} W_h[\max\{0; T_h^{in} - T^P\} - \max\{0; T_h^{out} - T^P\}]$$

$$Q_H \ge z_H^P(\psi)$$

$$g(\omega,\psi,y) \le 0$$

$$h(\omega,\psi,y) = 0$$

Here, the variables are defined as follows:

ψ = Set of variables in the reaction–separation–energy network
ω = Set of external flowsheet parameters
Q_H, Q_C = Heating and cooling utility loads

c_H, c_C = Cost coefficient for utility loads
w_H,w_C = Heat capacity flow rates for hot and cold streams, respectively
C_{sep} = Total separation cost
T_h^{in}, T_h^{out} = Inlet and outlet temperatures respectively for hot stream h
t_c^{in}, t_c^{out} = Inlet and outlet temperatures respectively for cold stream c
F_i = Total mass flow rate at element i
$F_{c,exit}$ = Mass flow rate of component c at reactor exit
z_H^p = Heating deficit above the pinch

The objective function Γ is a function of the variables within the unified reactor model and the heating and cooling utility loads. The cost model for separation presented in the previous section is incorporated within Γ as C_{sep}. The operating costs for the separation profile (for example, heat loads in the case of distillation) are directly incorporated into the energy minimization formulation. Note that this formulation combines the energy target in (P10) with the separation target in (P12).

The solution to formulation (P14) gives us an optimal network for the reactor flow configuration shown in Fig. 18. However, this flow model may not be sufficient for the synthesis problem, and we need to check for any other reactors that will help us improve the objective function. Using the approach developed in previous sections, we check for the same CSTR extensions from the solution to our unified reactor targeting model. Thus, in addition to the constraints in (P14), we add the CSTR extension constraints in (P11) and define $\Gamma^{(2)}$ as the objective with the same form as that in (P14). Here, $\psi^{(2)}$ is the set of new variables in the reactor energy network; this includes all the variables within ψ, the new variables X_{CSTR}, T_{CSTR}, and τ_{CSTR}, and the corresponding heat-exchange variables for cooling/heating the stream in the CSTR. There are no additional separation variables, since separation is confined to the segregated-flow component of this system. If the optimal solution to this formulation is $\Gamma^{(2)*} \geq \Gamma^*$, we have a reactor extension that improves the objective function. The next step consists of creating the new convex hull of concentrations and checking for any further extensions that improve the objective function within the flowsheet constraints. As before, we continue this procedure until there are no further reactor extensions that improve the objective function.

C. Example Problem

In this section, we reconsider the van de Vusse process to illustrate our synthesis approach. This example also shows the application of the unified reaction–separation–energy integration model. Comparisons are made between sequential and simultaneous modes of synthesis, and the applicability of the simplified model is verified.

Here, we devise a reaction separation network featuring energy integration for the following system using the proposed targeting scheme.

$$\begin{array}{ccccc} A & \xrightarrow{k_1} & B & \xrightarrow{k_2} & C \\ {\scriptstyle k_3}\downarrow & & & & \\ D & & & & \end{array}$$

The feed to the plant consists of pure A. This is mixed with the recycle gas stream, consisting of almost pure A, and preheated (C1) before entering the reactor. The flowsheet in Fig. 12 shows the reaction separation network followed by final separation columns to obtain product streams containing pure B and a C–D mixture. The volatilities of components in the network are given in the following descending order: [A, B, C, D]. The operating costs of the distillation columns (reboiler and condenser duties) are directly incorporated into the energy integration formulation and the columns are modeled in the same way as those in Section V. The reactor here is modeled by the discretized targeting model as shown in Fig. 16, with eight finite elements in the collocation procedure. The discretization procedure results in a total of 18 candidate hot streams and 11 candidate cold streams within the reaction separation network. The objective here is to maximize the total profit given by

$$J = 30F_B - 18F_{CD} - 6.95 \times 10^{-4}\tau F_0 - 4.566F_B(1 + 0.01(T^{in}_{H15} - 320)) - 7(F_B + F_{CD}) - 2F_{A0} - C_{sep} - 0.07Q_C - 0.8Q_H$$

In this expression, F_B, F_{CD} represent the production rates of B and CD, respectively, and F_{A0} is the amount of fresh feed. The first term corresponds to the product value, while the second term corresponds to the cost of waste treatment for undesired products C and D. The third term corresponds to the reactor capital cost, while the fourth and the fifth terms correspond to the recycling costs. The costs incurred for maintaining a desired separation profile, C_{sep}, is given in (P14).

The operating costs of the columns are directly incorporated into the energy network in terms of condenser and reboiler heat loads. We assume that the cost of the reactor can be described by the total residence time and is independent of the type of reactor. This can be justified on the grounds that the capital cost of the reactor itself is usually orders of magnitude smaller than the operating costs and the capital costs of the downstream processing steps. A target production rate of 960,000 lb/day is assumed for the desired product B.

Here, we consider two alternatives. First, we consider the sequential reaction and separation approach, where we force all the separation fractions to split only fractions. In the second case, we solve the above problem with the formulation proposed in (P14). In this case, the reaction–separation system and the energy network are optimized simultaneously. Table II presents a comparison between

TABLE II
RESULTS FOR SEQUENTIAL AND SIMULTANEOUS FORMULATIONS

	Reaction followed by separation	Simultaneous reaction and separation
Overall profit	53.87×10^6 \$/year	202.33×10^6 \$/year
Hot utility load	3.20×10^5 BTU/h	2.13×10^5 BTU/h
Cold utility load	131.120×10^6 BTU/h	126.799×10^6 BTU/h

the solutions obtained for simultaneous reaction separation and sequential reaction and separation. The results clearly show that by considering simultaneous reaction and separation as an option within the network, significant increases in overall profit can be obtained for this system.

As shown in Fig. 19, the separation profiles indicate removal of B and CD as reaction progresses, while retaining A for the complete residence time of 0.45 s. The temperature profile is a falling one as long as B and CD remain in the reactor. At every point where B and CD are separated out of the reactor, the temperature rises. This is because, as long as there is only A, a high reaction rate is desired to minimize reactor volume. However, as more B is produced, the temperature profile falls so as to reduce the excessive degradation of B to product C. Thus, the optimal temperature profile in this case is a nonmonotonic one. Also, among the 8 finite elements used in the discretization, only the candidate streams corresponding to 6 elements are active, since at the end of the sixth element, all molecules leave to the reactor exit ($t = 0.45$ s), as shown by the separation profile in Fig. 20. Furthermore, of the 18 candidate hot streams and 11 candidate cold streams, only 12 hot streams and 6 cold streams were active in the optimal network. Also, from the solution of the reactor extension problem, no reactor extensions are observed that improve the objective function for both sequential and simultaneous formulations.

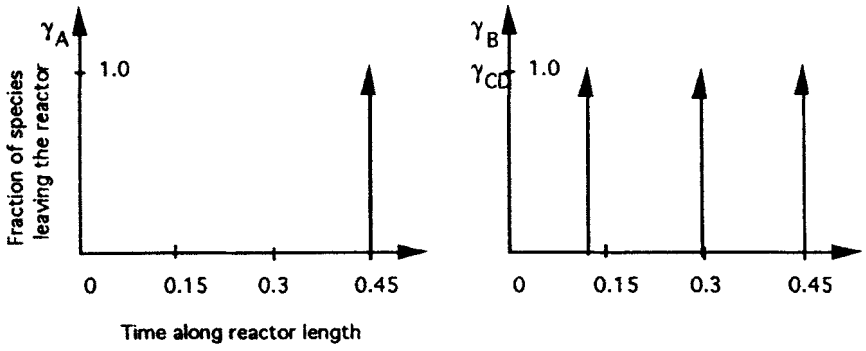

FIG. 19. Separation profiles along reactor length (simultaneous case).

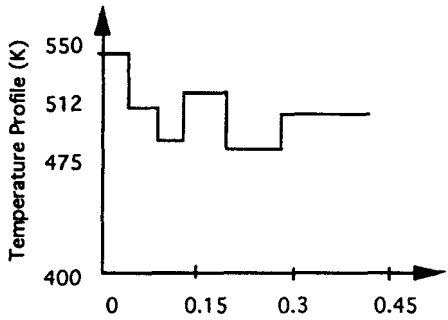

FIG. 20. Temperature profile (simultaneous case).

VII. Summary and Conclusions

In this paper we have addressed the development of mathematical programming strategies for the optimal synthesis and flowsheet integration of chemical reactor networks. Our discussion develops new methodologies for three major aspects of the reactor synthesis problem. These include optimal reactor network synthesis, energy integration of reactor networks, and the development of a combined reaction–separation–energy integration framework for overall synthesis.

In reactor network synthesis approaches based on superstructure optimization, the limitations stem from solutions that may be local or nonunique and that are only as rich as the superstructure chosen. To address these issues, geometric approaches based on attainable region (AR) concepts have recently been developed. Here, a region in concentration space is constructed that cannot be extended with further mixing and/or reaction. Hence, this region includes the concentation trajectories of all possible reactor networks for this system. This geometric approach leads to important insights into the structure of the optimal network. However, as construction of the attainable region is currently based on graphical tools, finding the AR is limited to two- or three-dimensional problem representations.

The synthesis approach proposed in this paper addresses the drawbacks of the superstructure and graphical AR techniques through a constructive, optimization-based targeting methodology. This targeting approach proceeds through the development of simplified reactor models and applies the concept of ARs to verify the sufficiency of these models. Our targeting approach is based on successively generating points of the feasible region for the reaction system with optimization over the convex hull of these points. We started with the segregated-flow limit to this model, which can be solved through a linear programming simplification. The example problems in Section III and in Balakrishna

and Biegler (1992a) indicate that, in many cases, the segregated-flow model is sufficient to describe the network. Sufficiency conditions also allow us to evaluate the suitability of the target obtained from the segregated-flow model. When the segregated-flow model is not sufficient, simple nonlinear programs can be solved to enhance the target. Here, each nonlinear program corresponds to a reactor extension from the convex hull of concentrations generated from the previous model, and this procedure is continued until there are no reactor extensions that improve the objective. With this stagewise approach, we therefore solve simpler models and verify their sufficiency in a stagewise manner.

The extension of this approach to nonisothermal systems follows similarly from the above approach. The main difference here is that temperature is an additional control profile and we consider schemes for maintaining a desired temperature profile. We accomplish this by postulating a cross-flow reactor model as the initial targeting model, since this allows for temperature control through feed mixing. From the convex hull of the concentrations available through the cross-flow reactor, we solve small nonlinear programming problems to generate reactor extensions that improve the objective function. In contrast to isothermal synthesis, the variable temperature profile in the initial cross-flow representation itself encompasses a large choice for the AR. In fact, while previous approaches have derived results by placing constraints on the temperature profiles, we show that for suitable temperature profiles, the conversion can asymptotically approach a stoichiometric upper bound for some systems. This is illustrated by the Lee–Aris sulfur dioxide oxidation, where the extent of reaction asymptotically approaches the upper bound, for a temperature profile shown in Section IV.

Reactor network synthesis in isolation, however, fails to address the interaction of the reactor design on the other process subsystems within the flowsheet. For example, reactors are associated with significant heat effects and our targeting approach allows for the integration of the reactor target with synthesis schemes for energy networks. The integration of our reactor targeting formulation with an energy targeting scheme, based on minimum utility costs (Duran and Grossmann, 1986), provides a general formalism for synthesizing energy integrated reactor networks. The results on the example problem indicate that significant increases in profit can be obtained by considering the two subsystems within a unified framework. Also, owing to high reaction exothermicities in the example, the heat-exchanger network is very flexible, as described in Section V.

Finally, we consider a preliminary approach for the optimal synthesis of reactor–separation systems. Here, we formulate a combined reaction–separation model by postulating a species–dependent residence time distribution. The optimization of this distribution function leads to a separation profile as a function of time along the reactor. The costs for maintaining a separation profile are handled through a separation index, which models the intensity of separation,

and a fixed charge modeled by binary variables for separation between any two components in the system. The reaction–separation model is then integrated with an energy targeting approach, and is implemented within our targeting framework. Results from a small example illustrate that the flowsheet performance indices can be enhanced significantly by considering reaction–separation systems, in contrast to the more conventional sequential reaction and separation.

While our targeting approach leads to an efficient, systematic strategy for synthesis of integrated reactor networks, there are still many open questions for targeting approaches. These can be summarized in terms of further development of geometric concepts, refinement of optimization strategies, and further extension and application to the design of new and existing processes. These topics are briefly summarized below.

Concepts for the construction of two- and three-dimensional regions have been firmly established by the work of Glasser, Hildebrandt and co-workers. For higher-dimensional systems, Hildebrandt and Feinberg (1992) have established a number of properties that lead to useful insights for processes with reaction and mixing, as well as additional rate processes. However, constructive procedures for higher-dimensional attainable regions still need to be developed. Similarly, optimization formulations still need to be refined in order to exploit the concepts of higher-dimensional ARs. This work presents simple formulations for constructing ARs consisting of PFRs, CSTRs, and some DSRs. However, improved formulations are still needed in order to provide "nonmonotonic" improvements in the network, as observed in Example 3. Moreover, many of the relationships that characterize the existence of DSRs and other connectors in higher-dimensional ARs need to be incorporated within optimization formulations.

Related to the development of AR concepts is the application of more powerful optimization formulations and algorithms. A current limitation to our targeting approach is the application of *local* optimization algorithms to nonconvex problem formulations, even though the resulting AR formulations demand global solutions. Clearly the development and application of efficient global optimization algorithms is still needed. A summary of the state of the art for global optimization in process synthesis is given by Floudas and Grossmann (1994). A related problem is the incorporation of uncertainty into the synthesis of reactor networks. Since reaction rate laws are often uncertain and the process needs to operate under a variety of conditions, it is important that the reactor network be flexible and robust to process changes and uncertain parameters. This problem has yet to be addressed for reactor network synthesis, even though systematic approaches have been developed for other process systems (see Grossmann and Straub, 1991, for a comprehensive survey). For reactor networks, this problem is complicated by the nonlinear character of the process as well as the large problem size.

Finally, further extensions of reactor network targeting include the design of reactive separation processes. Spurred by industrial successes (Agreda *et al.*, 1990), the strong integration of reaction and separation processes can lead to significant improvements and savings in the design of new processes. Section VI presents a preliminary approach for identifying the potential for coupling these two processes, but detailed phenomena have not been included in this approach. Again, the nonlinearity and complexity of the reaction and phase equilibrium models make this problem very difficult. Nevertheless, as with the generation of ARs, geometric insights (e.g., by Barbosa and Doherty, 1988) should lead to simplification of the synthesis procedure as well as refinement of the optimization formulation. In addition to reaction/separation systems, reactor network targeting can be applied to a number of design problems, particularly for the synthesis of waste-minimizing flowsheets. Here, the approaches described in this paper can be applied directly to these problems simply by considering waste generation as part of the design objective. Lakshmanan and Biegler (1994) recently considered this problem and established trade-offs in reactor targeting between process profitability and waste generation.

In conclusion, further development and application of reactor network targeting concepts will change the nature of current chemical process design and focus more attention on the integration of the reaction system and other process subsystems. This will lead to a better quantitative understanding of these systems and their trade-offs and ultimately will lead to processes that are more environmentally benign, more profitable, and less wasteful of raw materials, capital, and energy.

Acknowledgments

This work was supported by the Engineering Design Research Center, an NSF sponsored Engineering Research Center at Carnegie Mellon University, and by the Department of Energy.

References

Achenie, L. E. K., and Biegler, L. T. "Algorithmic Synthesis of Chemical Reactor Networks Using Mathematical Programming," *Ind. Eng. Chem. Fundam.* **25,** 621 (1986).

Achenie, L. E. K., and Biegler, L. T. "Developing Targets for the Performance Index of a Chemical Reactor Network," *Ind. Eng. Chem. Res.* **27,** 1811 (1988).

Achenie, L. E. K., and Biegler, L. T. "A Superstructure Based Approach to Chemical Reactor Network Synthesis," *Comput. Chem. Eng.* **14**(1), 23 (1990).

Agreda, V. H., Partin, L. R., and Heise, W. H. "High Purity Methyl Acetate via Reactive Distillation," *Chem. Eng. Prog.* **86**(2) (1990).

Andrecovich, M. J., and Westerberg, A. W. "An MILP Formulation for Heat Integrated Distillation Sequence Synthesis," *AIChE J.* **31,** 363 (1985).

Aris, R. "The Optimal Design of Chemical Reactors." Academic Press, New York, 1961.

Balakrishna, S. Ph.D. Thesis, Carnegie-Mellon University, Pittsburgh, PA (1992).

Balakrishna, S., and Biegler, L. T. "A Constructive Targeting Approach for the Synthesis of Isothermal Reactor Networks," *Ind. Eng. Chem. Res.* **31,** 300 (1992a).

Balakrishna, S., and Biegler, L. T. "Targeting Strategies for the Synthesis and Heat Integration of Nonisothermal Reactor Networks," *Ind. Eng. Chem. Res.* **31,** 2152 (1992b).

Balakrishna, S., and Biegler, L. T. "A Unified Approach for the Simultaneous Synthesis of Reaction, Energy and Separation Systems," *Ind. Eng. Chem. Res.* **32,** 1372 (1993).

Barbosa, D., and Doherty, M. F. "The Simple Distillation of Homogeneous Reactive Mixtures," *Chem. Eng. Sci.* **43,** 541 (1988).

Chitra, S. P., and Govind, R. "Synthesis of Optimal Serial Reactor Structure for Homogenous Reactions. Part II: Nonisothermal Reactors," *AIChE J.* **31**(2), 185 (1985).

Cuthrell, J. E., and Biegler, L. T. "On the Optimization of Differential Algebraic Process Systems," *AIChE J.* **33,** 1257 (1987).

Douglas, J. M. "A Hierarchical Decision Procedure for Process Synthesis," *AIChE J.* **31,** 353 (1985).

Douglas, J. M. "Conceptual Design of Chemical Processes." McGraw-Hill, New York, 1988.

Duran, M. A., and Grossmann, I. E. "Simultaneous Optimization and Heat Integration of Chemical Processes," *AIChE J.* **32,** 123 (1986).

Dyson, D. C., and Horn, F. J. M. "Optimum Distributed Feed Reactors for Exothermic Reversible Reactions," *J. Optim. Theory Appl.* **1,** 1 (1967).

Fjeld, M., Asbjornsen, O. A., and Aström, K. J. "Reaction Invariants and the Importance of in the Analysis of Eigenvecters, Stability and Controllability of CSTRs," *Chem. Eng. Sci.* **30,** 1917 (1974).

Floudas, C. A., and Grossmann, I. E. "Global Optimization for Process Synthesis and Design," *in* "Foundationns of Computer-Aided Process Design (FOCAPD '94), Snowmass, CO" (L. T. Biegler and M. F. Doherty, eds.), p. 198 (1994).

Fogler, H. S. "Elements of Chemical Reaction Engineering." Prentice-Hall, Englewood Cliffs, NJ, 1992.

Froment, G. F., and Bischoff, K. B. "Chemical Reactor Analysis and Design." Wiley, New York, 1979.

Glasser, B., Hildebrandt, D., and Glasser, D. "Optimal Mixing for Exothermic Reversible Reactions," Paper 70g, *Annual AIChE Meeting,* Chicago (1990).

Glasser, B., Hildebrandt, D., and Glasser, D. "Optimal Mixing for Exothermic Reversible Reactions," *Ind. Eng. Chem. Res.* **31**(6), 1541 (1992).

Glasser, D., Crowe, C. M., and Jackson, R. "Zwietering's Maximum-Mixed Reactor Model and the Existence of Multiple Steady States," *Chem. Eng. Commun.* **40,** 41 (1986).

Glasser, D., Crowe, C. M., and Hildebrandt, D. "A Geometric Approach to Steady Flow Reactors: The Attainable Region and Optimization in Concentration Space," *Ind. Eng. Chem. Res.* **26**(9), 1803 (1987).

Godorr, S., Hildebrandt, D., and Glasser, D. "The Attainable Region for Mixing and Multiple Rate Processes," *Chem. Eng. J.* (1994).

Grossmann, I. E., and Straub, D. A. "Recent Developments in Evaluation and Optimization of Flexible Chemical Processes," *Proc. COPE '91,* p. 41 (1991).

Hartmann, K., and Kaplick, K. "Analysis and Synthesis of Chemical Process Systems." Elsevier, Amsterdam, 1990.

Hildebrandt, D. Ph.D. Thesis, University of Witwatersrand, Johannesburg, South Africa (1989).

Hildebrandt, D., and Biegler, L. T. "Synthesis of Chemical Reactor Networks," *in* "Foundations of Computer-Aided Process Design (FOCAPD '94), Snowmass, CO" (L. T. Biegler and M. F. Doherty, eds.), p. 52 (1994).

Hildebrandt, D., and Feinberg, M. "Optimal Reactor Design from a Geometric Viewpoint," Paper 142c, AIChE Annual Meeting, Miami Beach, FL (1992).

Hildebrandt, D., and Glasser, D. "The Attainable Region and Optimal Reactor Structures," *Proc. ISCRE Meet.*, Toronto (1990).

Hildebrandt, D., Glasser, D., and Crowe, C. "The Geometry of the Attainable Region Generated by Reaction and Mixing: With and Without Constraints," *Ind. Eng. Chem. Res.* **29**(1), 49 (1990).

Horn, F. "Attainable Regions in Chemical Reaction Technique," *in* "Third European Symposium on Chemical Reaction Engineering," Pergamon, London, 1964.

Horn, F. J. M., and Tsai, M. J. "The Use of Adjoint Variables in the Development of Improvement Criteria for Chemical Reactors," *J. Optim. Theory Appl.* **1**(2), 131 (1967).

Jackson, R. "Optimization of Chemical Reactors with Respect to Flow Configuration," *J. Optim. Theory Appl.* **2** (4), 240 (1968).

Kokossis, A. C., and Floudas, C. A. "Synthesis of Isothermal Reactor-Separator-Recycle Systems," *Annual AIChE Meeting*, San Francisco (1989).

Kokossis, A. C., and Floudas, C. A. "Optimization of Complex Reactor Networks. I. Isothermal Operation," *Chem. Eng. Sci.* **45**(3), 595 (1990).

Kokossis, A. C., and Floudas, C. A. "Synthesis of Non-isothermal Reactor Networks," Annual AIChE Meeting, Los Angeles, CA (1991).

Kramers, H., and Westerterp, K. R. "Elements of Chemical Reactor Design and Operation," Academic Press, New York, 1963.

Kravanja, Z., and Grossmann, I. E. "Prosyn—An MINLP Synthesizer," *Comput. Chem. Eng.* **14**(12), 1363 (1990).

Lakshmanan, A., and Biegler, L. T. "Reactor Network Targeting for Waste Minimization," presented at National AIChE Meeting, Atlanta, GA (1994).

Lee, K. Y., and Aris, R. "Optimal Adiabatic Bed Reactors for Sulphur Dioxide with Cold Shot Cooling," *Ind. Eng. Chem. Process Des. Dev.* **2,** 300 (1963).

Levenspiel, O. "Chemical Reaction Engineering," Wiley, New York, 1962.

Linnhoff, B., and Hindmarsh, E. "The Pinch Design Method for Heat Exchanger Networks," *Chem. Eng. Sci.* **38,** 745 (1983).

Narasimhan, G. "Optimization of Adiabatic Reactor Sequence with Heat Exchanger Cooling," *Br. Chem. Eng.* **14,** 1402 (1969).

Nishida, N., Stephanopoulos, G., and Westerberg, A. W. "Review of Process Synthesis," *AIChE J.* **27,** 321 (1981).

Omtveit, T., and Lien, K. "Graphical Targeting Procedures for Reactor Systems," *Proc. Eur. Symp. Comput-Aided Eng. (ESCAPE-3)*, Graz, Austria, *1993* (1993).

Paynter, J. D., and Haskins, D. E. "Determination of Optimal Reactor Type," *Chem. Eng. Sci.* **25,** 1415 (1970).

Pibouleau, L., Floquet, P., and Domenech, S. "Optimal Synthesis of Reactor Separator Systems by Nonlinear Programming Method," *AIChE J.* **34,** 163 (1988).

Ravimohan, A. "Optimization of Chemical Reactor Networks with Respect to Flow Configuration," *J. Optim. Theory Appl.* **8**(3), 204 (1971).

Trambouze, P. J., and Piret, E. L. "Continuous Stirred Tank Reactors: Designs for Maximum Conversions of Raw Material to Desired Product," *AIChE J.* **5,** 384 (1959).

van de Vusse, J. G. "Plug Flow Type Reactor vs. Tank Reactor," *Chem. Eng. Sci.* **19,** 994 (1964).

Viswanathan, J. V., and Grossmann, I. E. "A Combined Penalty Function and Outer-Approximation Method for MINLP Optimization," *Comput. Chem. Eng.* **14,** 769–782 (1990).

Waghmere, R. S., and Lim, H. C. "Optimal Operation of Isothermal Reactors," *Ind. Eng. Chem. Fundam.* **20,** 361 (1981).